THE APPLICATION OF COMMERCIAL OBSERVATION SATELLITE IMAGERY FOR THE VERIFICATION OF DECLARED AND UNDECLARED PLUTONIUM PRODUCTION REACTORS

Hui Zhang*
Frank N. von Hippel

PU/CEES Report No. 319

August 1999

Center for Energy and Environmental Studies
Princeton Environmental Institute
Princeton University
Princeton, NJ 08544-5263
(609) 258-5445
www.princeton.edu/~cees

Hui Zhang is a Visiting SSRC-MacArthur Foundation International Research on Peace and Security Post-doctoral Fellow.

The Application of Commercial Observation Satellite Imagery for the Verification of Declared and Undeclared Plutonium Production Reactors

Hui Zhang and Frank N. von Hippel

ABSTRACT

Negotiations on a Fissile Material Cutoff Treaty (FMCT) will soon be underway at the Committee on Disarmament in Geneva, and will include detailed attention to how such a treaty could be verified. This paper explains how commercial observation satellites can be effective in verifying that reactors used to produce weapons plutonium in the past are kept in a shutdown status under a cutoff treaty or moratorium. The satellites considered are the new-generation satellites with fine spatial resolution images in the visible and near infrared band complemented by thermal infrared images with lower-spatial resolution but good temperature resolution. These satellites can also contribute to the detection of undeclared nuclear-reactor sites and suspicious construction activities.

Introduction

After several years delay, due to debates over its scope and linkage to nuclear disarmament measures, negotiations on a Fissile Material Cutoff Treaty (FMCT) may finally be launched at the Geneva Conference on Disarmament in 2000.[1] Under the FMCT, the eight nations which have not joined the Nonproliferation Treaty as non-weapons states (the U.S., Russia, Britain, France, China, Israel, India and Pakistan) would end production of nuclear-weapons-useable fissile material except under international safeguards , which would assure non-diversion to weapons use. However, four of the eight (the U.S., Russia, Britain and France) have already announced that they have ended their production for weapons of plutonium and highly-enriched uranium (HEU)[2] and China has privately communicated that it has not been producing these materials for weapons since approximately 1991. It can be hoped that other nations may join in this fissile materials production moratorium.[3]

Although any reactor with significant power can be used to produce plutonium[4] and virtually any mix of plutonium isotopes can be used to make nuclear explosives,[5] most plutonium for weapons appears to have been produced in dedicated production reactors (see table 1). In some cases these reactors have been dual-purpose, producing electric power as well as plutonium. In some cases they have been used to produce other isotopes besides plutonium and neutron beams for research purposes. One isotope produced in significant quantities for nuclear-weapons purposes is tritium.[6] But, in most cases, plutonium-production reactors have been shut down when countries have halted production.

---

[1] See http://www.acronym.org.uk.

[2] Uranium enriched to greater than 20 percent U235.

[3] See e.g. by Steven Fetter and Frank von Hippel, "A Step-by-Step Approach to a Global Fissile Materials Cutoff," *Arms Control Today 25, #8* (October 1995), pp. 3-8.

[4] The burnups used to produce "weapon-grade plutonium" (plutonium containing about 6% Pu-240 in the U.S.) are on the order of 1 gram of fission in one kg of fuel in natural-uranium fueled production reactors. At these burnups, about 0.8 grams of plutonium are produced per gram of fission. One gram of fission produces about one megawatt-day of heat. A production reactor operating at an average power of 30 MWt would therefore produce 8 kg of plutonium per year, a "significant quantity" according to IAEA standards, i.e. enough to make a first-generation (Nagasaki-type) nuclear weapon.

[5] J. Carson Mark, "Explosive Properties of Reactor-grade Plutonium," *Science & Global Security 4* (1993), pp. 111-128.

[6] Tritium a radioactive isotope of hydrogen with a half-life of 12.1 years, has a fusion reaction with at a temperature of about 4 keV. It is used in nuclear weapons to produce neutrons to initiate the chain reaction in a supercritical mass of fissile material and also can be used later on to produce extra neutrons to "boost" the power of the fission explosion.

The purpose of this paper is to explain how the shutdown of reactors can often be confirmed using commercial observation satellites, i.e. without intrusive, on-site inspections. A companion paper will discuss the possibilities for similarly detecting evidence of the shutdown of gaseous-diffusion uranium-enrichment plants.[7]

---

[7] Hui Zhang and Frank von Hippel, "Verification that Uranium Enrichment Facilities are Not Operating Using Commercial Observation Satellites" (working title), to be published.

Table 1. Plutonium-production reactors of the world and their cooling systems

Reactors	Reactor Type[a]	Status	Peak Power (GWt)	Cooling System
UNITED STATES				
Hanford Reservation				
8 Reactors: B,D,F,DR,H & C KW & KE	LWGR	Permanently shutdown:[b] and partially dismantled	2.5 4.4	Once through; hot water discharged into Columbia River
N-Reactor	LWGR	Dual use (electric power), startup 12/31/63; in cold standby since1987, deactivation initiated.	4	"
Savannah River Site				
K reactor	HWR	In cold standby since 1988 with no plans for operation, startup: 10/51	2.71	Natural draft hyperbolic cooling tower
Reactors: P R	HWR	Permanently shutdown[c]	2.68 2.26	Both reactors discharged their hot water into a cooling pond
Reactor: C L	HWR	"	2.915 2.7	Once-through cooling: hot water discharged into Savannah River through streams and swamps

[a] LWGR: Light-water cooled, graphite-moderated reactor; HWR: Heavy-Water Reactor.

[b] Operating dates: B (9/44-2/12/68), D (12/44-6/26/67), F (2/45-6/25/65), DR (10/50-12/30/64), H (10/49-4/65), C(11/52-4/25/69); KW(1/55-2/1/70), KE(4/55-1/28/71).

[c] Operating dates: P (2/54-1989) R (12/53-6/15/64); C (3/55-1989), L-reactor (7/54-2/18/68)

RUSSIA

Sites	Reactor Type	Status	Peak Power (GWt)	Cooling system
Ozersk (Chelyabinsk-65)				
5 Reactors: A IR AV-1, AV-2 & AV-3	LWGR	Permanently shutdown[d]	 0.5 0.065 2.09	All with once through cooling, discharge into Lake Kyzyltash
Seversk (Tomsk-7)				
3 Reactors: I-1, I-2 &ADE-3	LWGR	Permanently shutdown[e]	2	I-1 reactor: once-through cooling, discharge into the Romashka Creek and then Tom River; ADE-3, 5: natural draft hyperbolic cooling towers
2 Reactors: ADE-4, ADE-5	LWGR	Operating since 65 and 68: producing heat and electricity for Seversk and Tomsk	2	Natural draft hyperbolic cooling towers
Zhelenznogorsk (Krasnoyarsk-26)				
Reactors: AD, ADE-1	LWGR	Permanently shutdown[f]	2	Once through cooling with Yenisey River cooling water
Reactor: AD-2	LWGR	Operating since 64; producing heat and electricity for Zhelenznogorsk	2	The secondary cooling loop uses once-through Yenisey River cooling water.

[d] Operating dates: A (6/22/48-87), IR (12/22/51-5/24/87), AV-1 (7/15/50-8/12/89), AV-2 (4/6/51-7/90), AV-3 (9-15/52-11/1/90).
[e] Operating dates: I-1 (11/20/55-8/21/90), I-2 (9/58-12/28/90), ADE-3 (7/14/61-8/14/92).
[f] Operating dates: AD (9/25/58-6/30/92), ADE-1 (7/20-61-9/29/92)

UNITED KINGDOM

Site	Reactor Type	Status	Peak Power (GWt)	Cooling system
Sellafield				
2 Windscale Piles		Being decommissioned,[g] operated 1951-57	-	
4 Calderhall reactors	GCR	Operable, dual use(electric power)[h]	0.24	Natural draft hyperbolic cooling towers
Chapelcross				
4 Chapelcross reactors	GCR	Operable, dual use(electric power)	0.24	"

FRANCE

Marcoule complex				
G1,G2, G3 reactors	GCR	G1 and G2 decommissioned; G3 permanently shutdown[i]	-	-
Celestin-1,2 reactors	HWR	Alternating in operation; producing only tritium since 1991; operating since 67, 68	-	-
Others				
Chinon A1,2,3	GCR	permanently shutdown[j]	-	-
Bugey1	GCR	permanently shutdown, operated 71-??	-	-
St.LaurentA1,2	GCR	permanently shutdown, operated 69-?,71-?	-	-
Phénix	FBR	operating since 74	-	-

[g] http://www.ukaea.org.uk/oindex.htm

[h] Calder Hall reactors began full-power in 10/56, 2/57, 5/58, and 2/59; Chapel Cross reactors in 2/59, 9/59, 11/59, and 3.60. See also http://www.bnfl.com/BNFLWebSite.nsf/HTML/CompanyProfile?OpenDocument

[i] Operating dates: G1 (56-10/68), G2 (59-80), G3 (59-84)

[j] Operating dates: Chinon 1 (61-73), Chinon 2 (65-??), Chinon 3 (67-??)

CHINA

Site	Reactor Type	Status	Peak Power (GWt)	Cooling system
Jiuquan Complex				
Jiuquan reactor	LWGR	shutdown; operated 66-91?	≤0.5?	six natural draft hyperbolic cooling towers
Guangyuan Complex				
Guangyuan reactor	?	shutdown; operated ??-91?	≤ 1?	?

ISRAEL

Dimona Complex				
Dimona reactor	HWR	In operation since 12/63	≤0.07?	Mechanical draft cooling tower

Site	Reactor Type	Status	Peak Power (GWt)	Cooling system
INDIA				
Bhabha Atomic Research center				
Cirus reactor	HWR	In operation since 60	0.04	Once through into bay
Dhruva reactor	HWR	In operation since 8/8/85; also produces neutron beams and radioisotopes for research and medicine	0.1	"
PAKISTAN				
Khushab reactor	HWR?	In operation since 1999?	-	Once-through to Jhelum River?

Sources: Thomas B. Cochran, William M. Arkin, Robert S. Norris, and Milton M. Hoenig, *U.S. Nuclear Warhead Facility Profiles* (Ballinger, 1987); Thomas B. Cochran, Robert S. Norris, and Oleg Bukharin, *Making the Russian Bomb: From Stalin to Yeltsin* (Westview, 1995); David Albright, Frans Berkhout and William Walker, *Plutonium and Highly Enriched Uranium 1996* (Oxford, 1997); *NUKEM Market Report: World Nuclear Capacity*, December 1993; also see http://www.insc.anl.gov/nre/nre.html; see http://www.fas.org/nuke/guide/.

Capabilities of the new generation of commercial satellites

Visible and near-infrared. The capabilities of commercial observation satellites are being greatly improved, starting in 1999 with the launch of a new generation of commercial satellites with one-meter spatial resolution at visible wavelengths and several days revisit time (see Table 2). Although still an order of magnitude less capable than military imaging satellites,[8] the resolutions of these new satellites will be an order of magnitude better than the 10-30 meter resolution of previous generation commercial observation satellites such as France's SPOT and the U.S. Landsat 4 and 5 whose capabilities for treaty verification have already been examined in previous studies.[9] A brief history of commercial observation satellites and a more detailed discussion of their relevant capabilities may found in Appendix A.

Table2. Present and planned commercial satellites with high resolution in visible and near-infrared (VNIR) wavelengths [See Appendix A for sources.]

Satellite System	Owning Country	Launch Date	Res.[10](m) Pan/Mult[11]	Revisit Time (days)	Swath Width (km)	Max. View Angle (degrees)	Orbit Altitude (km)
KVR-1000	Russia	1987	5	-14	-	-	200
Iris-1C,1D	India	1995,7	5.8	5	70	26	817
Spin-2	Russia	1990s	2	-	2,10,40	-	220
IKONOS	U.S.	99 (failed)	1/4	1-4	11	26	681
QuickBird	U.S.	1999?	1/4	1-5	27	30	600
OrbView	U.S.	1999?	1,2/4	3	8	45	460
EROS-A	Israel	1999?	2	3	14	45	480
EROS-B	Israel	2001?	1	1	20	45	600

[8] U.S. KH-12 satellites, first launched in November 1992, can reportedly achieve 10cm-resolution images in the visible. They also carry thermal infrared (TIR) imaging systems. If the TIR system uses the same optical system, its resolution could be as good as 2 meters. See http://www.fas.org/spp/military/program/imint/kh-12.html.

[9] M. Krepon, et. al., Commercial observation satellites and international security, (St. Martin's Press, Inc., New York,1990); M. Slack and H. Chestnutt, Open skies--technical, organizational operational, legal and political aspects, (York University, Canada,1990); M. Krepon, et. al., Open skies, arms control, and cooperative security, (St. Martin's Press, Inc New York,1992).

[10] Instanteous field of view of pixel.

Although we have no images of nuclear facilities as yet from the new high-resolution commercial satellites, a larger number of older images of such facilities with comparable resolution have recently become available as a result of the declassification of CORONA panchromatic satellite images taken by the U.S. KH-4 intelligence satellites during the period 1967-72.[12] The spatial resolutions of these images – especially towards the end of this period -- are comparable to those expected from of high-resolution commercial satellites.

Thermal infrared. High-resolution images of 1m in the visible and near infrared are very useful for identifying nuclear sites and facilities and indirect evidence of their operation, such as plumes of vapor rising from cooling towers. However, thermal infrared (TIR) imaging is directly sensitive to temperature differences. Unlike VNIR, TIR images can be taken in nighttime as well as daytime. On the other hand, TIR generally has a much lower spatial resolution because of the longer wavelengths involved. Objects with temperatures below 100 ^{0}C emit dominantly at wavelengths above 8μm.TIR measurements are therefore taken within the 8-14μm atmospheric transmission "window" thus involving wavelengths 20 times longer than visible wavelengths, which center around 0.5 microns. To achieve the same resolution from a given altitude would correspondingly require an aperture 20 times larger.

Table 3. Satellites with TIR (8-14$_\mu$m) Sensors

Satellite	Country	Launch date	TIR Resol (m)	Temp. Accuracy(°K)	Altitude (km)	Swath width(km)	Revisit time(days)
Landsat-5	USA	1984	120	0.5- 1	705	185	16
Landsat-7	USA	4/15/99	60	0.5-1	705	185	16
Aster	USA/Japan	1999?	90	0.2	-	60	16

Measuring absolute temperatures accurately with TIR requires difficult corrections for atmospheric transmission. However, the most useful information for verification purposes is usually the difference between the temperature of an object of interest and its surroundings. The

[11] Panchromatic/ multispectral

thermal sensitivity of TIR instruments for *relative* temperature measurement is referred to as the temperature "accuracy" here (see Table 3).

The only existing commercial satellites with TIR satellites are Landsat --5 and Landsat-7. Landsat-5, which was launched in 1984, carries two imaging sensors, the Multispectral Scanner(MSS) and the Thematic Mapper (TM). The Thematic Mapper, which operates in the thermal infrared region in the spectral range of 10.4-12.5 μm, has spatial resolution of 120 m and an absolute sensitivity of 8 °K. Based on its TIR images, its relative temperature accuracy is possible about 0.5-1 °K.[13] Landsat-7, which was launched on April 15, 1999, carries the Enhanced Thematic Mapper Plus (ETM+) which has an improved spatial resolution of 60 m.[14] We assume that it has the same temperature accuracy as Landsat-5.

A second new satellite with TIR is the Advanced Spaceborne Thermal Emission and Reflection Radiometer (ASTER) was originally scheduled to be launched in 1998 but has been delayed. It is expected to launch in 1999 soon.[15] ASTER is jointly funded by the U.S. National Air and Space Administration (NASA) and Japan's Ministry of International Trade and Industry as part of the Earth Observing System constellation of satellites. It has five TIR bands covering the spectral range from 8.125 μm to 11.65 μm at a spatial resolution of 90m. The absolute temperature sensitivity around 270 -340 °K is 1 °K and the relative temperature accuracy is 0.2 °K.

Monitoring the shut-down status of production reactors with commercial satellites at visible wavelengths

Most U.S., Russian, and French plutonium production reactors have been shut down. The U.S. and Russia have a still-to-be-fully implemented agreement under which they have agreed to bilaterally monitor the status of their shutdown reactors and to confirm that new plutonium produced by three Russian plutonium- production reactors which still operate to generate heat

---

[12] See e.g. http://www.fas.org/nuke/guide/russia/facility/nuke/index.html.
[13] T. M. Lillesand and R. Kiefer, Remote sensing and image interpretation, (John Wiley & Sons, Inc., 1994); G.E.Wukelic, et al., "Radiometric Calibration of Landsat Thematic Mapper Thermal Band", Remote Sens.Environ.28:339(1989).
[14] See http://ls7pm3.gsfc.nasa.gov

and electric power is not diverted to weapons use. Britain still operates eight small plutonium-production reactors to generate electrical power and tritium and France still operates the Phénix demonstration breeder reactor which may in the past have produced plutonium for weapons. However, all plutonium separation activities in the Britain and France are now subject to Euratom and IAEA safeguards.

China has not announced specifically that it has shut down its plutonium-production reactors but reportedly shut down at least one in 1984 before it reportedly suspended plutonium-production for weapons in 1991. In the future, Israel, India and/or Pakistan may shut down reactors currently producing plutonium for weapons. It is therefore interesting to try to answer the question: For shutdown reactors not subject to international monitoring, how could other countries verify non-intrusively that they had really been shut down?

While the reactor is operating and for a time after shutdown, removal of heat from the reactor core is essential to prevent a meltdown of the reactor fuel. A variety of cooling systems for dissipating the waste heat into the environment exist, including the use of cooling towers, cooling ponds and once-through condenser cooling with river or seawater.[16] Table 1 lists the cooling systems of plutonium-production reactors, as far as we have been able to determine them. Below we show how the operation of different types of cooling systems can be monitored by commercial observation satellites.

Reactors with cooling towers. Cooling towers for reactors are classified according to the method used for heat transfer from the cooling water in the reactor's closed primary or secondary coolant circuit to the air and the method utilized to create air movement through the tower.[17] Most cooling towers are "wet," which means that their primary heat-removal mechanism is through the vaporization of externally-supplied water on heat-exchange surfaces. The cooling water requirement for wet-type cooling towers is much smaller than for once-through cooling systems.[18] For this reason, reactors with wet-type cooling towers can be located at a distance from large water bodies. In a dry tower, heat is transferred to air without the addition of water vapor. However, a significantly larger cooling tower is required for a

---

[15] See http://asterweb.jpl.nasa.gov/asterhome.

[16] Kam W.Li and A.Priddy, Power Plant System Design, (John Wiley&Sons,1985).

[17] J.Weisman,R.Eckart, Modern Power Plant Engineering, (Prentice-Hall, Inc.,1985).

[18] The evaporation of a kilogram of water from at 25 °C absorbs about 2.4 Mj. The warming of a kg of water by

given cooling capacity. [19]

In both cases, air circulation through the tower results, at least in part, from the buoyancy of the heated air, which creates a chimney effect. Towers that rely solely on this buoyancy effect are classified as natural-draft towers. When large fans are used to increase the airflow through the tower, the tower is classified as a mechanical draft tower. It will be seen from table 1 that, for production reactors with cooling towers, wet-type, natural draft hyperbolic cooling towers are mostly used.[20] A group of such towers associated with four of Britain's dual-purpose production reactors is shown in Figure 1.

It will be seen from the figure that natural-draft hyperbolic cooling towers are very large: several tens of meters in height and more than 10 meters in diameter at the top. It should be very easy to identify such a large structure using a 1-m resolution satellite images.

When a cooling tower is operating, a water-vapor plume will be seen emerging from its top (see Figure 2). Since the air is saturated after it passes through wet packing at the base of the tower and the water cools as it rises through the tower, it is supersaturated when it emerges. Downwind from the tower the air mixes with cooler ambient air. How far downwind the mix remains supersaturated depends upon the saturation of this ambient air (see Appendix B). In any case, a plume should always be visible from above at the exit of the tower. Since the diameter of the tower exit is on the order of ten meters, the plume should be easy to detect with a 1m-resolution satellite images. Since it requires at least several weeks irradiation to produce a practical concentration of plutonium in reactor fuel,[21] the revisit time of several days for current commercial satellites should be adequate for detection of operation. Much shorter revisit times will, of course, be possible when there is a constellation of such satellites.

Figure 3 shows an image taken by a CORONA satellite on 15 Sept.1971[22] of two of the five production reactors then operating at the Siberian Chemical Combine (Tomsk-7). All except the first of these reactors (I-1) were equipped with natural-draft hyperbolic cooling

---

10 °C absorbs only two percent as much heat: 42 kj.

[19] Heating a kg of dry air at 20 °C by 10 °C absorbs 10 kj. Adding water to keep it saturated requires the evaporation of 12 grams of water, absorbing an additional 28 kj.

[20] It will be seen that only Israel is known to be using a mechanical-draft cooling tower.

[21] For a commercial light water power reactor, the typical specific power is about 30MWt per metric ton of fuel. Production reactors usually have much lower specific powers. Achieving a typical burnup of 1000 MWd/Mt to produce weapon-grade plutonium would therefore require more than 33 days.

[22] See http://www.fas.org/nuke/guide/russia/facility/nuke/index.html.

towers. The diameters of the tower tops is about 30 meters.[23] The ground resolution in this panchromatic image is about 1.8m.[24] The six towers at the upper left and the eight towers at the bottom right are, in all likelihood, allocated to the EI-2 and ADE-3 reactors respectively. EI-2 operated from Sept 1958 to Dec 1990 at an average thermal power output of approximately 1200 MWt and produced about 10 tons of WgPu. ADE-3 operated from July 1961 to Aug 1992 at an average thermal power output of approximately 1900 MWt and produced about 14 ton WgPu.[25] The physical structures of the cooling towers, and the vapor plumes at their tops can be clearly seen. The clarity of a commercial satellite image with a 1-m pixel resolution would be comparable. Therefore we conclude that a 1m-resolution commercial satellite could monitor the shutdown status of reactors with cooling towers. It might also be possible to monitor the frequency of shutdown of power reactors equipped with cooling towers. Since the fuel in power reactors is irradiated too much higher burnups than for production reactors operated so to produce weapon-grade plutonium,[26] frequent shutdowns would raise suspicions.

---

[23] Private communication, Oleg Bukharin, ,Center for Energy and Environmental Studies, Princeton University,1999.

[24] From the recent declassified collection of KH-1 to KH-6 photos for the period 1960 to 1972. This photo was taken by the KH-4B satellite. A directory to these photos was shown on the U.S. Geological Service web site at http://edcwww.cr.usgs.gov/glis/hyper/guide/disp.

[25] Nils Bohmer and Thomas Nilsen, Seversk(Tomsk-7) (Bellona Working Paper, No.4,1995). David Albright,et al.,Plutonium and Highly Enriched Uranium 1996-World Inventories, Capabilities and Policies, (Oxford University Press,1997).

[26] The burnup required to produce weapon-grade uranium in natural-uranium fueled production reactors is about 1000 MWt-days/ton. Power reactors are designed to fission most of the U-235 in their fuel. This corresponds to burnups of about 7000 MWt-days/ton for natural-uranium-fueled power reactors and 30,000-60,000 MWt-days/ton for reactors fueled with 3-6 percent enriched uranium.

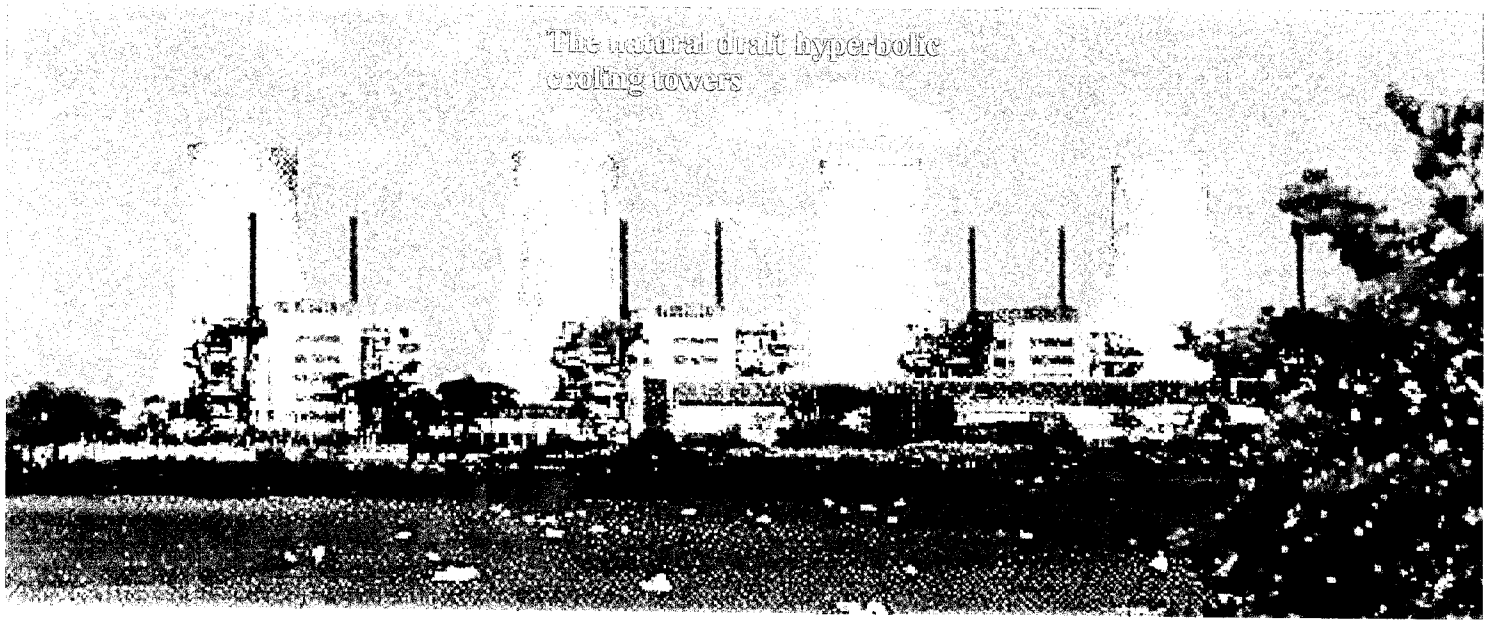

Fig.1 The natural-draft hyperbolic cooling towers of the four Chapelcross reactors in Southern Scotland. These carbon-dioxide cooled reactors were formerly used to produce plutonium for U.K nuclear weapons between 1959 and 1964, and later used to produced tritium. They also produce electric power. Their initial design ratings were 180MW thermal and 42 MW-electric, later up-rated to 240 MWth and 54 Mwe(now 50 MWe) .
Sources: http://www.fas.org/nuke/guide/uk/facility; http://www.insc.anl.gov/nre/; David Albright,et al, Plutonium and Highly Enriched Uranium 1996- World Inventories, Capabilities and Policies, SIPRI,1997.

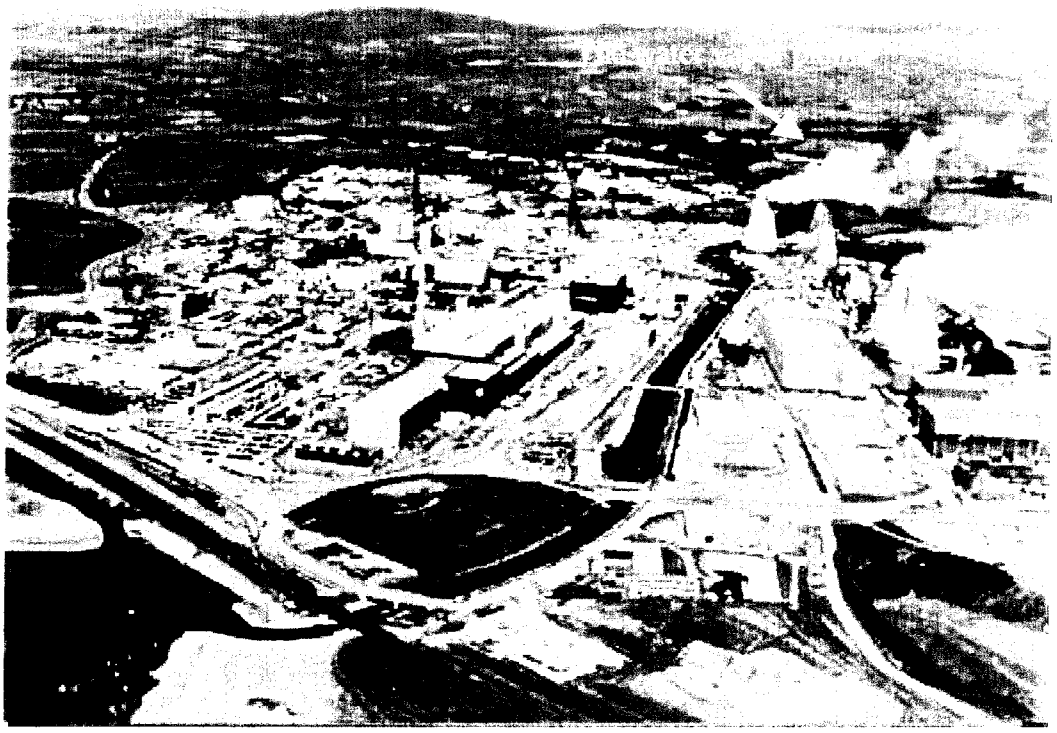

Fig.2 The four Calderhall Magnox reactors at Sellafield, U.K.
The picture shows the four huge natural draft hyperbolic cooling towers of the reactors and the water-vapor plumes. These four reactors made a significant contribution to UK plutonium for weapons. They entered service between October 1956 and May 1959. They also produce electric power. Their initial design ratings were 180MW thermal and 42 MW-electric, later up-rated to 240 MWth and 54 MWe (now 50 MWe).

Sources:http://www.fas.org/nuke/guide/uk/facilit/; http://www.insc.anl.gov/nre/; David Albright,et al, Plutonium and Highly Enriched Uranium 1996- World Inventories, Capabilities and Policies, SIPRI,1997.

Fig.3 Declassified U.S. Corona Satellite Image of Site of Plutonium Production Reactors I-1,EI-2 and ADE-3 at Tomsk-7, Russia. Corona Mission 1115-1, 15Sept 1971, KH-4B system, 6ft spatial resolution. The cooling towers and the water vapor plume over the towers are clearly visible.

Fig.4 Declassified U.S. Corona Satellite Image of Dimona Nuclear Facilities in Israel.(Missiom1115-2,29 September 1971,KH-4B system with 6ft(1.8m) spatial resolution). The containment of Israel's production reactor is clearly identifiable, as is a mechanical cooling tower.
Source: http://www.fas.org/irp/imint/4_dim_03.htm.

Reactors with a cooling pond or once-through cooling supplied from a river. Some production reactors, such as the P and R reactors at the Savannah River Site, have used cooling ponds in which the water which cools the reactor directly or indirectly is cycled through a pond from whose surface the heat is dissipated via evaporation, convection and radiation.[27] In other cases, a "once-through" system is used in which water is withdrawn from a river and discharged downstream or is drawn from a lake or estuary so large that the temperature of the intake water is not significantly affected by the hot-water discharged by the reactor.

Reactors with a once-through cooling system supplied by rivers often have a holding pond where the cooling water is pumped before being treated and pumped through the reactor. These holding ponds can also be used for emergency cooling water if the pumps from the river fail. Figure 5 shows a triplet of holding ponds in front of the L-reactor at the U.S. Savannah River Site.[28] If such a holding pond or a cooling pond were to dry up, that would be a good indication that the reactor was shut down. This could be easy to detect by 1m resolution VNIR images from the change in the reflectivity of pond. This is illustrated by Figure 6, a CORONA KH-4B photograph with an 1.8m resolution taken in 1969. This photo shows three huge ponds near the Jiuquan nuclear complex in China. The two dark ponds on the left appear to contain water while the one on the right appears dry.

However, it should be noted that only in dry climates such as that in the Jinquan area will holding ponds dry out when not in use. In a wet area such as the Savannah River site ,where rainfall exceeds the rate of evaporation, the pools will remain full unless a drain is opened.

---

[27] Kam W.Li and A.Priddy, Power Plant System Design, (John Wiley&Sons,1985).
[28] Thomas B.Cochran,et al.,Nuclear Weapons Databook, Vol.III:U.S.Nuclear Warhead Facility Profiles,(Ballinger,1984).

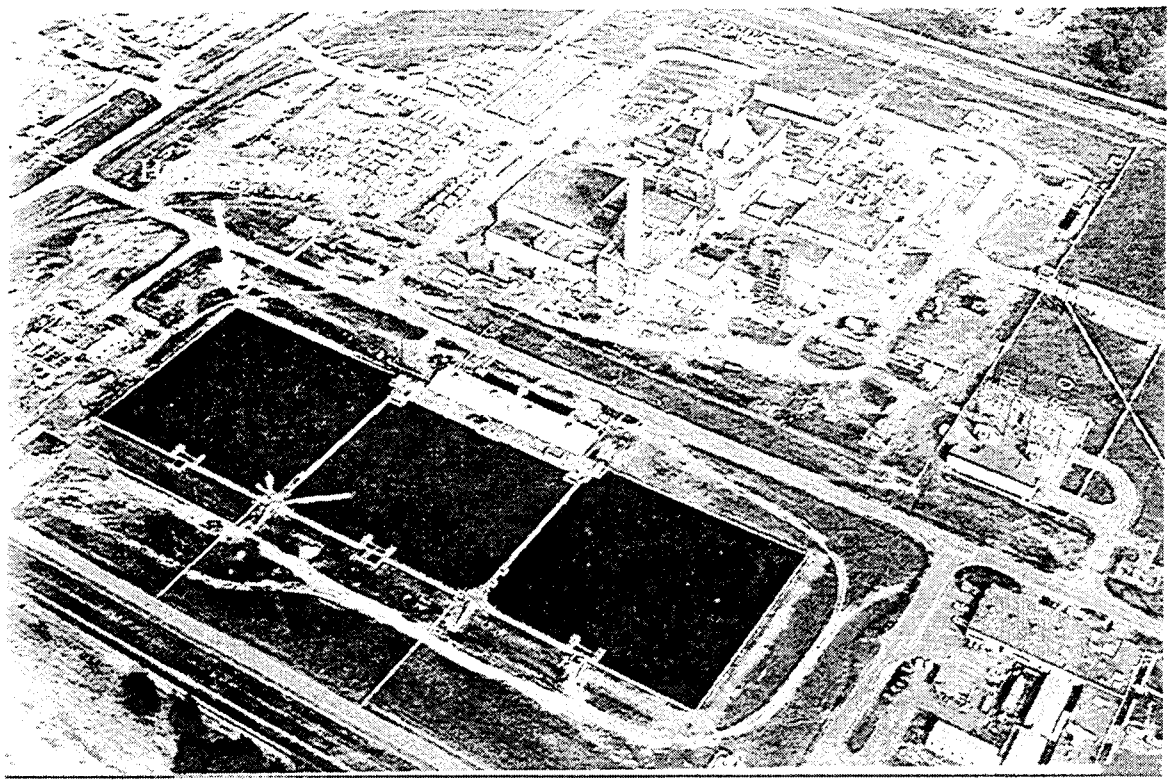

Fig.5 L-Reactor at Savannah River Site, U.S. In front of the reactor are three holding ponds for cooling water.

Source: Thomas B. Cochran, William M. Arkin, Robert S. Norris and Milton M. Hoenig, Nuclear Weapons Databook, Volume III: U.S. Nuclear Warhead Facility Profiles, (Ballinger, 1984).

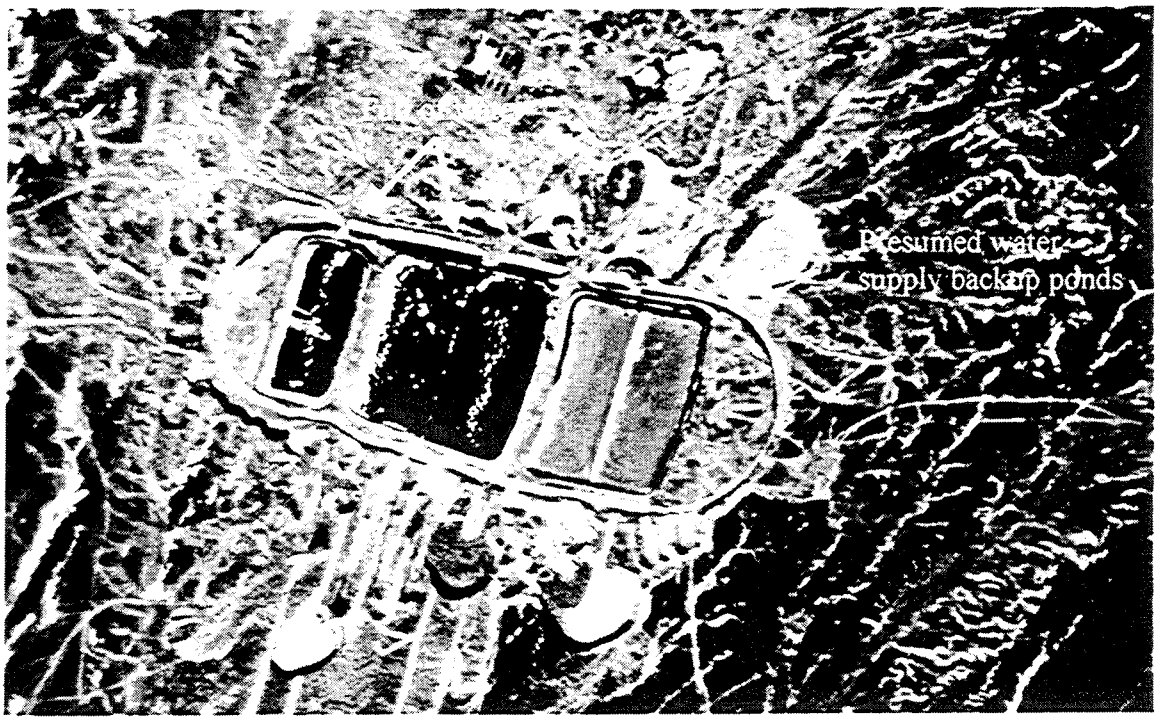

Fig.6 A Declassified U.S. Corona Satellite image. Corona Mission 1108-1 on 9 Sept 1969, KH-4B system with 6 ft resolution. The huge three ponds are nearby the Jiuquan Reactor. It is presumed the water supply backup ponds for the reactor. The satellite image show clear whether the ponds with water or not. The deep black parts have water.

Monitoring the shut-down status of production reactors with commercial satellites at thermal-infrared wavelengths.

Thermal-infrared (TIR) sensors can detect small temperature differences but, because of their relatively poor spatial resolution, the objects that they detect have to be either very large or hot enough so that they significantly raise the temperature in one or more pixels(see Appendix C).

Reactors with Cooling Ponds: A cooling pond is a body of water in which the cooling water dissipates its heat into the atmosphere through radiation, convection, conduction and evaporation. [29]

Cooling ponds require a large surface area because they have a low heat transfer rate. It is generally estimated that, to dissipate 1000 MW thermal requires about 2-8 km^2 of surface area.[30] Such large areas are easily imaged, even with the poor spatial resolutions of the TIR instruments described in Table 3.

We estimate the required area per GWth of power as

$$A/P = \ln r/K = (\ln r)/[K\Delta T] \quad km^2/MW \qquad (1)$$

Here K is the heat transfer coefficient from the water to air and space (by radiation), typically in the range 20-40 Watts/km^2-°C, ΔT is the difference between the coolant discharge and intake temperatures and

$$r \equiv (T_d - T_e)/(T_i - T_e)$$

where T_e is the equilibrium temperature of the cooling pond surface if the power plant were not operating.

Consider as an example, the case of the cooling pond for Chernobyl Nuclear Reactor Site (Figure 7). Assume K = 30 Watts/m2-^{0}C, and summer values for T_d, T_i and T_e of 35, 25 and 20 ^{0}C respectively, i.e. r = 3 and ΔT = 10 °C. Substituting in Eqn. 1 gives A/P = 2.4 km^2/GWth.

There were four reactor units on the site, sometimes operating simultaneously. The electricity output for each unit was about 1000Mwe and the conversion efficiency of heat into

---

[29] Ref.16.

[30] L.C.Wilbur, Handbook of Energy System Engineering: Production and Utilization, (John Wiley &

electricity was about 33 percent. The cooling pond therefore was designed to dissipate up to about 8000MWth. For the values of K, r and $T_d - T_i$ that we have assumed , the area of the cooling pond calculates from Eq.(1) is about 20 km^2, which is roughly consistent with Fig.7, obtained with the Landsat TIR imager which shows the surface temperature distribution in the cooling pond before and after the April 26, 1986 accident.[31]

Sons,1985).

[31] "United States Army Multispectral Imagery Product Guide", Second Edition, ATC-IA-2681-030-94, May 1994.

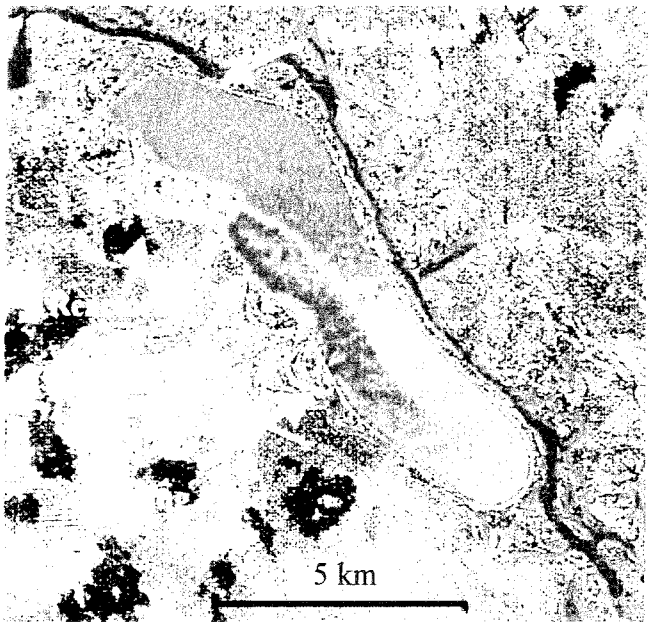

Fig.7a

Fig.7b

Fig.7 Landsat-5 TIR images of Chernobyl Nuclear Reactor Site, Ukranine. Fig.7a was taken on 22April1986 when the reactor was in normal operation. Fig.7b was taken on 8May1986 when the reactor was at suspended operation. Source: " United States Army Multispectral Imagery Product Guide", Second Edition, ATC-IA-2681-030-94, May 1994.

Reactors with once-through cooling systems. Some production reactors have "once-through" cooling in which water from a river, large lake or the ocean is used for cooling and then discharged back into to the river downstream of the intake or into the lake or ocean in a way to assure that it will not be taken back into the intake before it has cooled to near equilibrium temperatures. Figure 8 shows a TIR thermal pattern obtained from an aircraft flying at an altitude of 1.2 km of the hot water discharges from the C and L reactors at the U.S. Savannah River Site through a swampy area next to the Savannah River.[32] The reactors operated at powers greater than 2.5 GWth. The streams of hot water are about 4 km long and cover an area of more than 0.5 km^2 at temperatures at least 5 °K higher than that of the river. The Hanford reactors discharged their hot water into the Columbia River; and India's Dhvrua and Cirus research reactors at Trombay discharge their hot water into a bay (see Fig. 9) . If the water body such as lake and bay are near at a steady-state and steady-flow condition, the thermal pattern of the discharged hot water around the outlet is similar to that of the cooling pond. Based on the estimate for the cooling pond, it can be expected that also the hot water would cover a large area, large enough for modern TIR commercial satellites to detect. In fact, even with the relatively poor resolution TIR images of Landsat-5 TM, the hot effluents discharged into the lakes and rivers from the reactors have been detected. This is shown, for example, by several Landsat-5 TIR images.

Fig. 10 shows two Landsat-5 TM images of the "Mayak" plutonium production complex at Ozersk (Chelyabinsk-65) in the Urals, acquired on 1 August 1987 and 13 May1993, acquired by Bhupendra Jasani et al.[33] Water from Lake Kyzyltash was used to cool the reactors. In the 1987 thermal image, a plume of warm water can be clearly seen extending north for a considerable distance along the eastern fringes of Lake Kyzyltash. The surface temperature of the water within this plume is a maximum of 10°C warmer than that of the bulk of water in the lake. In the 1993 thermal image of Lake Kyzyltash, the warm plume of effluent water is still evident, and is in fact larger in spatial extent and thermal magnitude, being a maximum of 15°C warmer than the bulk of water.

Figure 11 shows one Landsat-5 TM thermal image taken over Canadian Gentilly Nuclear

---

[32] Frank von Hippel,et al.," Stopping the Production of Fissile Materials for Weapons", Scientific American, September 1985, Vol.253, No.3.

[33] Bhupendra Jasani and Alan Blackburn, " Piercing into Secret Nuclear Establishment Using Imagery from Civil Satellites," in Proceedings of the 21st Annual Conference of the Remote Sensing Society, 11-14 Sept,1995,

Generating Stations on 15 April 1996,[34] when Gentilly-1 reactor was inactive and Gentilly-2 reactor was in operation. Gentilly-2 , a Candu type reactor with netput 860 MWe, discharges its hot water through an open cooling channel into the St.Lawrence River. The TIR image shows clearly a thermal plume leaving the channel.

As long as the warm water from the reactors is discharged into surface waters, an area of elevated temperatures around the discharge point should be detectable using satellite-borne TIR sensors. However, in theory at least a discharge might be concealed by releasing it through a long pipe with many holes along its length laid in deep water so that a mix results with a temperature which is not detectably warmer than that of the surface waters above. In Appendix D we calculate that, for a 15 °C temperature rise, the volume of a discharge carrying away 1 GWth would be 16 m^3/sec. To bring that temperature down to the 0.2 °C temperature rise detectable by Aster would require dilution by a factor of 75 to a volume of 1200 m^3/sec. For comparison, the flow past Krasnoyarsk of the Yenesei River, the largest River in Russia, is 5-10,000 m^3/sec.[35] The three underground nuclear reactors that discharged into the river nearby had a combined thermal power of up to 6 GW so, with perfect mixing, it might be possible to conceal their output from Aster. As table 1 shows, reactors with a capacity of only 0.06 GWth are strategically significant. There are quite a few rivers with one tenth the average flow of the Yenesei.

---

ed. Paul Curran and Colette Robertson.

[34] The picture is from " Potential Application of Commercial Satellite Imagery in International Safeguards," Final Report to the International Atomic Energy Agency(IAEA), Atomic Energy Control Board(AECB) Canadian Safeguards Support Programme and the Department of Foreign Affair and International Trade(DFAIT) International Security Research an Outreach Program, to be published for IAEA(id # IMS98031). The authors would like to thank Phillip Baines of DFAIT to provide the picture, and the Canadian Atomic Energy Control Board(AECB) ,the Department of Foreign Affair and International Trade(DFAIT) and the ImStrat Corporation for permission to use of the picture.

[35] The Krasnoyarsk dam is rated at 6 GWe. If the height is 100 meters, this corresponds to a flow at 90 % conversion efficiency of 7,000 m^3/sec.

Fig.8 The thermal infrared images show the discharges of hot water from two U.S. plutonium-production reactors at Savannah River,S.C. In this false-color representation the streams of hot water are red and orange; the cooler background is rendered in blue and gray. These images were made from an airplane flying at an altitude of 1.2 kilometers.
Source: Frank von Hippel, David H. Albright and Barbara G. Levi, "Stopping the Production of Fissile Materials for Weapons", Scientific American, September 1985,Vol.253, No.3 ,p41.

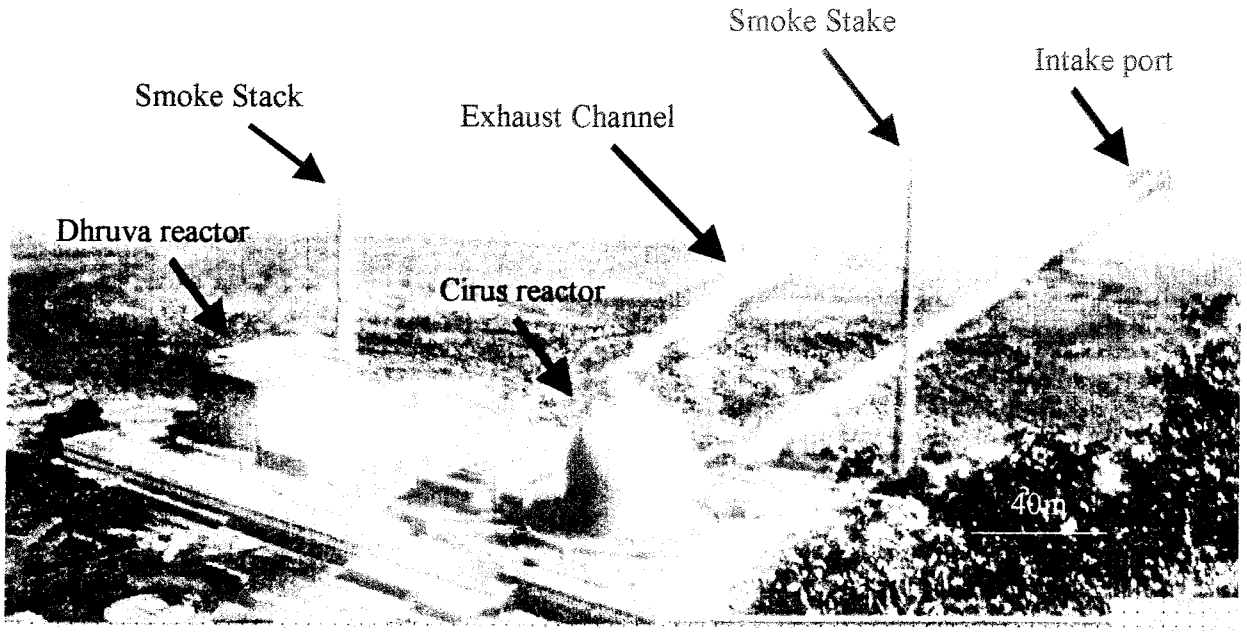

Fig.9 Dhruva and Cirus Research Reactors at Trombay, India.

The Cirus and Dhruva reactors use natural uranium fuel and a heavy water moderator. The 40 MWth Cirus reactor began operation in 1960; The 100 MWth Dhruva reactors started in August 1985. Both reactors produce plutonium for India's nuclear weapons. They are still in operation without IAEA safeguards. Source: Research Reactors at Trombay, Bhabha Atomic Research Center, Bombay-400 085, July 1987.

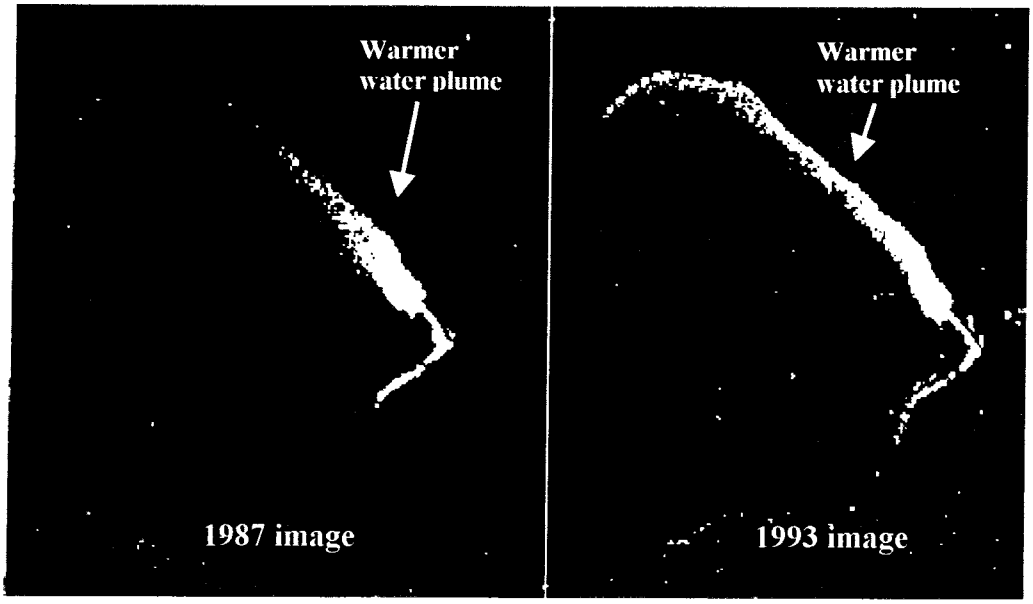

Fig.10 Discharges in Lake Kyzyltash from Mayak plutonium production reactors. The warmer water plume is clearly seen in 1987 and 1993 LandsatTM thermal images. Source:Bhupendra Jasani and Alan Blackburn, 'Piercing into Secret Nuclear Establishments Using Imagery from Civil Satellites,' in Proceedings of the 21st Annual Conference of the Remote Sensing Society, 11-14 September 1995,ed.Paul Curran , et al..

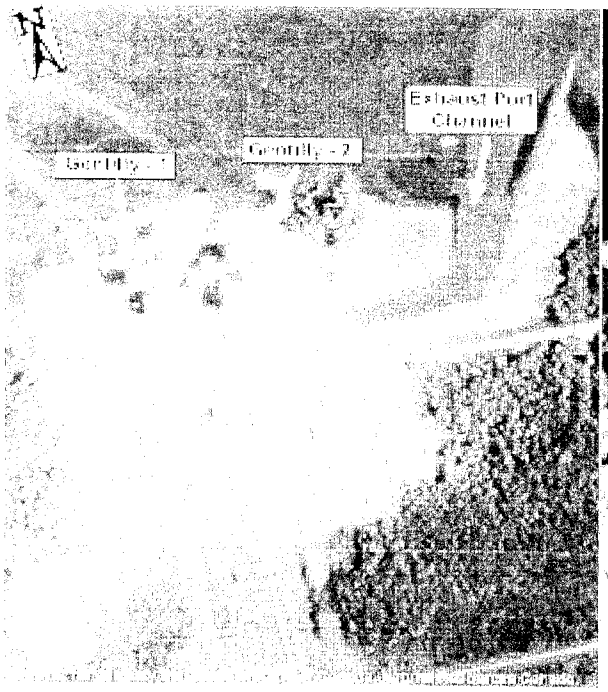

Fig.11a. Airphoto taken on 30 July 1977

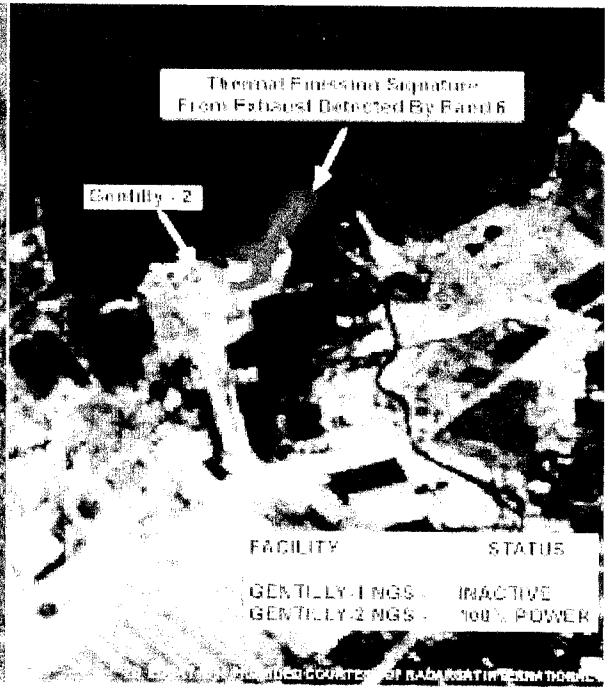

Fig.11b. Landsat-5 TM Image on 15 April,96
(Bands 6/1/2/3 Combination)

Fig11 Airphoto and Landsat-5TM False Colour Composite of Canadian Gentilly Nuclear Generating Stations. Source: " Potential Application of Commercial Satellite Imagery in International Safeguards," to be published for IAEA(id # IMS98031). See also ref.3[illegible].

Reactors with cooling towers: Although they have much poorer spatial resolution, TIR sensors, unlike VNIR sensors, can detect the warm plumes of water vapor emerging from cooling towers at night as well as during the day. The plumes are visible in TIR only in the same region where condensed droplets of water vapor make them visible to the eye, however. This is because, the water and air molecules in the invisible plume after the water droplets have evaporated radiate only at their characteristic molecular wavelengths which are generally reabsorbed by the same classes of molecules in the cooler higher atmosphere before the radiation can escape to be detected on a satellite. Some of the black body radiation emitted by the droplets in a visible vapor plume, by contrast, is emitted in the spectral "windows" in the 8-14 μm region between the molecular absorption bands and thereby can escape from the atmosphere.

The visible plume from a cooling tower is usually at least few degrees Centigrade warmer than the ambient air (see Appendix B). The size of the area it covers depends upon the humidity of the ambient area (see also Appendix B). If the size is comparable to the instantaneous field of view (IFOV) of a pixel in the TIR sensor and if it is also warmer than the ground below, the relative temperature difference should easily be detectable by the sensors on Landsat 5 and 7, which have relative temperature resolutions of better than one °C (see Table 3). If the size of the plume is smaller than the IFOV of a pixel, then its detectability depends on its relative temperature being high enough to drive the average effective relative temperature detected by the pixel above detection threshold (see Appendix C). The inability of the LandsatTM detectors to detect plumes from some towers is not surprising. A test was done by the Carnegie Endowment's Nonproliferation Project in which they requested an operating history for a 60MW research reactor operated at Brookhaven National Lab near New York City along with Landsat images taken of the reactor on two days, one when the reactor was operating, and one when it was shut down. This reactor uses closed-cooling towers (presumably wet-type cooling towers) to dissipate heat. The Landsat-5 TIR did not find convincing evidence of the thermal signature when the reactor was operating.[36] This result is consistent with our estimation given in appendix C.

We conclude that existing TIR on board satellite LandsatTM and ETM+ could be detect the

---

[36] See Leonard S.Spector,"Monitoring Nuclear Proliferation", in Commercial Observation Satellites and International Security, ed. Michael Krepon, et al.,Carnegie Endowment for International Peace,1990.

plume from the towers. Probability of detection will be high with high-resolution TIR satellite such as Aster.

Table 4. Monitoring the shutdown status of production reactors using new commercial satellite imagery

Cooling System	VNIR	TIR
Cooling towers	For an operating reactor, the water-vapor plume from the towers would be visible. (Primary indicator)	Existing TIR on board satellite LandsatTM and ETM+ could detect the plume from the towers. Probability of detection is high with high resolution TIR satellite such as Aster. (Secondary indicator)
Cooling Pond	When shutdown, the cooling pond can dry up in dry regions, which should be readily seen by new VNIR images. (Secondary indicator)	The elevated temperature of the surface of pond near the discharge point can be readily detected by new or existing TIR satellite imagery. (Primary indicator)
Once Through Cooling	Under shutdown status, large holding ponds for cooling water might dry out in dry climates, which could be readily observed. (Secondary indicator)	The hot water discharged into lake or river would be easily seen by new or existing TIR satellite imagery. (Primary indicator)

In summary (see also Table 4): 1) 1-m resolution VNIR satellite imagery can detect the water-vapor plumes from cooling towers – and it appears that, a fair fraction of the time, TIR sensors could as well; 2) for reactors with cooling ponds or once-through cooling systems, TIR imagery can detect the warm-water plume discharged into the receiving body of water unless rather elaborate concealment measures are taken. Overall, the shutdown status of most existing reactors should be readily detected by modern commercial satellite imagery

Detection of undeclared production reactors

To produce plutonium for weapons, a country could operate a dedicated, undeclared production reactor, and associated facilities. In the absence of elaborate concealment measures, such a reactor site could in principle be detected and identified using 1-m resolution VNIR satellites. This can be illustrated with Corona images of China's plutonium-production reactor site at Jiuquan Atomic Energy Complex (often referred to as Plant 404). This site, reportedly the first of China's two plutonium-production complexes, is located in Subei county in Gansu province.[37] The complex contained the reactor, a chemical separation plant, and a plutonium processing plant for refining plutonium metal. Construction of the reactor started around 1960. By the end of 1966, the reactor began to operate. It is a graphite-moderated water-cooled reactor, fueled with natural uranium. One group has estimated from published information that the Jiuquan reactor initially had a power of 250 MWth and that this capacity was doubled by the early 1980s.[38] According to a recent report, the Jiuquan plutonium production center was shutdown in 1984. It is also reported that the China is preparing to systematically decommission other major military nuclear material facilities, including facilities at the Guangyuan plutonium production complex.[39]

Recently declassified intelligence imagery, collected between 1960 and 1972, shows that U.S. CORONA photo-reconnaissance satellites began to target the Jiuquan complex at least as early as December 7, 1960 and thereafter took photos of this area frequently. Figure12a shows a declassified CORONA satellite image of the Jiuquan nuclear complex taken by a CORONA satellite on 30 May1972.[40] Figure12b, taken by a KH-4B satellite, shows an enlarged view of the Jiuquan reactor site. The physical structure of the six cooling towers can be seen clearly. Even their size can be estimated. Based on KH-4B system parameters, it is

---

[37] The second site, in Guangyuan county in Sichuan province, reportedly began operation in early the 1970s. where weapons plutonium has been produced (Robert S. Norris, et al.,*Nuclear Weapons Databook Volume V: British, French, and Chinese Nuclear Weapons,* Westview Press, 1994).

[38] David Wright, Lisbeth Gronlund and Ying Liu, Estimating China's Stockpile of Fissile Materials for Weapons, Draft, Union of Concern scientist Technical Working Paper, Washington,D.C. April; 1996.

[39] Mark Hibbs,"China said to be preparing for decommissioning defense plants," *Nuclear Fuel*, May17,1999.

[40] See http://www.fas.org/nuke/guide/china/facility/jiuquan.htm.

estimated that the inside diameter of the tower top is about 20 meters.[41]

Fig.12c shows a KH-4B CORONA satellite image of the Jiuquan reactor taken on December 9, 1969 when the sun was relatively low. The security perimeter fence and the high stack at the site can be identified clearly from their shadows, even though they are too narrow to be resolved themselves. The sun angle in combination with the length of the shadow can be used to obtain good estimates of the heights of the stack, cooling towers, and fences. The roads and railway at the site can also be seen in these images.

The reactor location can also be precisely determined using the locational information for these satellite images. The location of Jiuquan Atomic Energy Complex has been reported as 39.36N 94.58E.[42] However, from these recent declassified CORONA images, its location can be was found at 40.25N 97.35E, 300 km away.

From an initial study of these declassified CORONA satellite images, it is quite straightforward to identify characteristic features of a military plutonium-production reactor site: an isolated site, security perimeter, cooling towers denoting a large source of waste heat next to a relatively small building (which must therefore contain a major energy source), a high narrow stack for safe disposal of leaks of radioactive gases from failed fuel elements, a railroad track reflecting the presence of heavy equipment, and the absence of facilities for storage of coal, gas or oil or of high-tension power lines which would be present if the site were a commercial power plant.

---

[41] The reported best ground resolution is 1.8m in the panchromatic mode; the frame format of the film is approximate 2.18inch *29.8inch; the normal photo scale on film is 1:247,500; and normal ground coverage in an image frame is therefore about 14x190km.

[42] Robert S. Burrows et al., Nuclear Weapons Databook Volume V: British, French and Chinese Nuclear Weapon(Boulder, CO: Westview Press,1994).

Fig.12a Declassified U.S. Corona Satellite Images of Plutonium Production Reactor at Jiuquan Nuclear Complex, China. (Corona Mission 111-7 on 30 May 1972, KH-4B system, 6 ft spatial resolution)

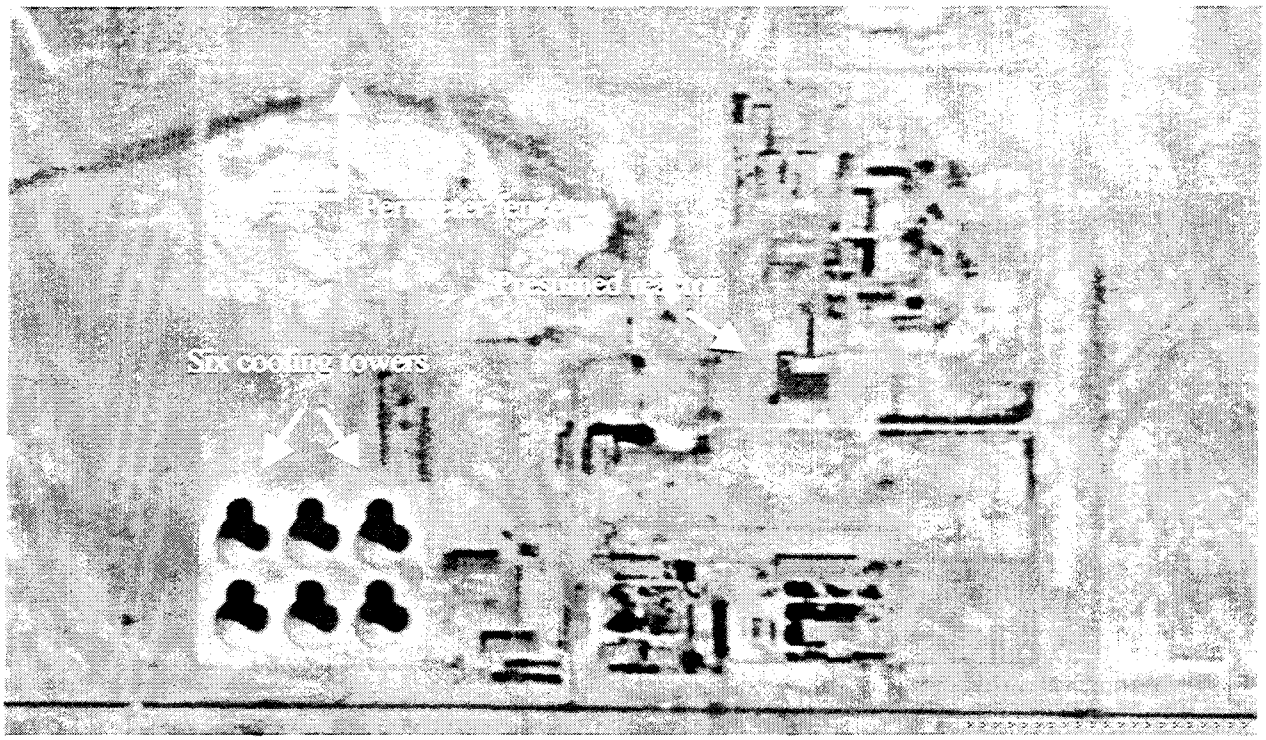

Fig.12b The Jiuquan plutonium production reactor. An enlarged view of the reactor area as shown in Fig.12a. The six natural draft hyperbolic cooling towers are readily seen.

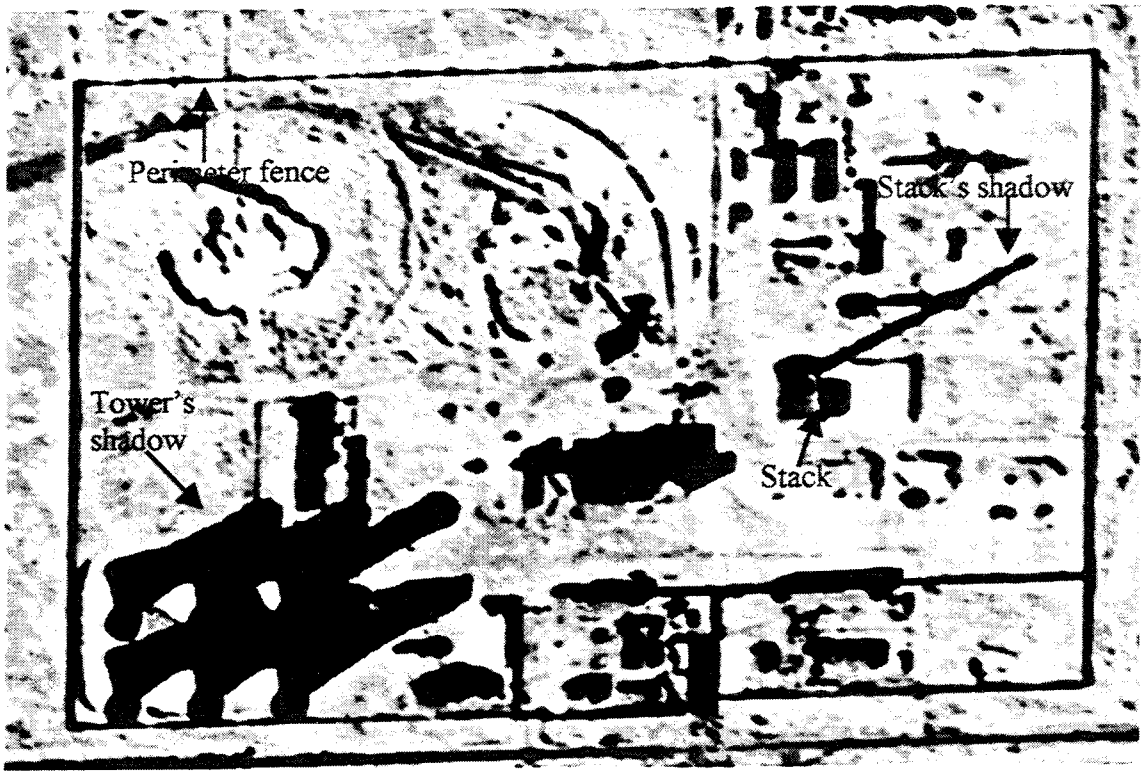

Fig.12c Declassified U.S. Corona Satellite Imagery of Jiuquan Reactor.(Corona mission 1108-1, 9 December1969). From this picture, the perimeter fence and high stack are made visible through their shadows.

The date when a facility was completed can also be determined retroactively by looking at a time series of images. Fig.13a is a CORONA image taken by KH-4A system on 7 October 7, 1965. Even with the 2.7-m resolution of this earlier satellite, one can clearly see that four cooling towers had been finished, and two were under construction. Fig.13b, a CORONA image taken by a KH-4B satellite on 18 September 1967 shows that all six cooling towers had been finished. This is consistent with the report that the Jiuquan reactor began its operation at the end of 1966. Of course, reactor construction includes a great many activities, such as the shipment of heavy components. Large trucks should be big enough to be identified in 1-m resolution VNIR images. Such activities would be present for a considerable period of time. It has been estimated that even the construction of a small, simple graphite-moderated, air-cooled 30 MWth production reactor able to produce about 9 kg -- or about one bomb's worth -- of plutonium per year), would take about 3 years to construct.[43]

Although satellite images can find the suspicious facilities or activities, they cannot make the final determination. The information they provide could be used to trigger on-site special inspections, however. For example, it was U.S. satellite photos taken around the declared nuclear sites at Yongbyon, North Korea that triggered the IAEA to request an inspection of two suspected waste sites and one building suspected to have been used for reprocessing activities near the Radiochemical Laboratory at Yongbyon.[44]

---

[43] U.S. Congress, Office of Technology Assessment, Nuclear proliferation and Safeguards, (New York,1977),pp.94-98.

[44] David Albright, "North Korea Plutonium Production," Science& Global Security,5:1(1994).

Fig.13a Declassified U.S. Corona Satellite Image of Jiuquan Reactor.
(Mission 1025-1, 7 October 1965,KH-4A system with 9ft (2.7m) spatial resolution). The absence of shadows for two cooling towers shows that they were still under construction in 1965.

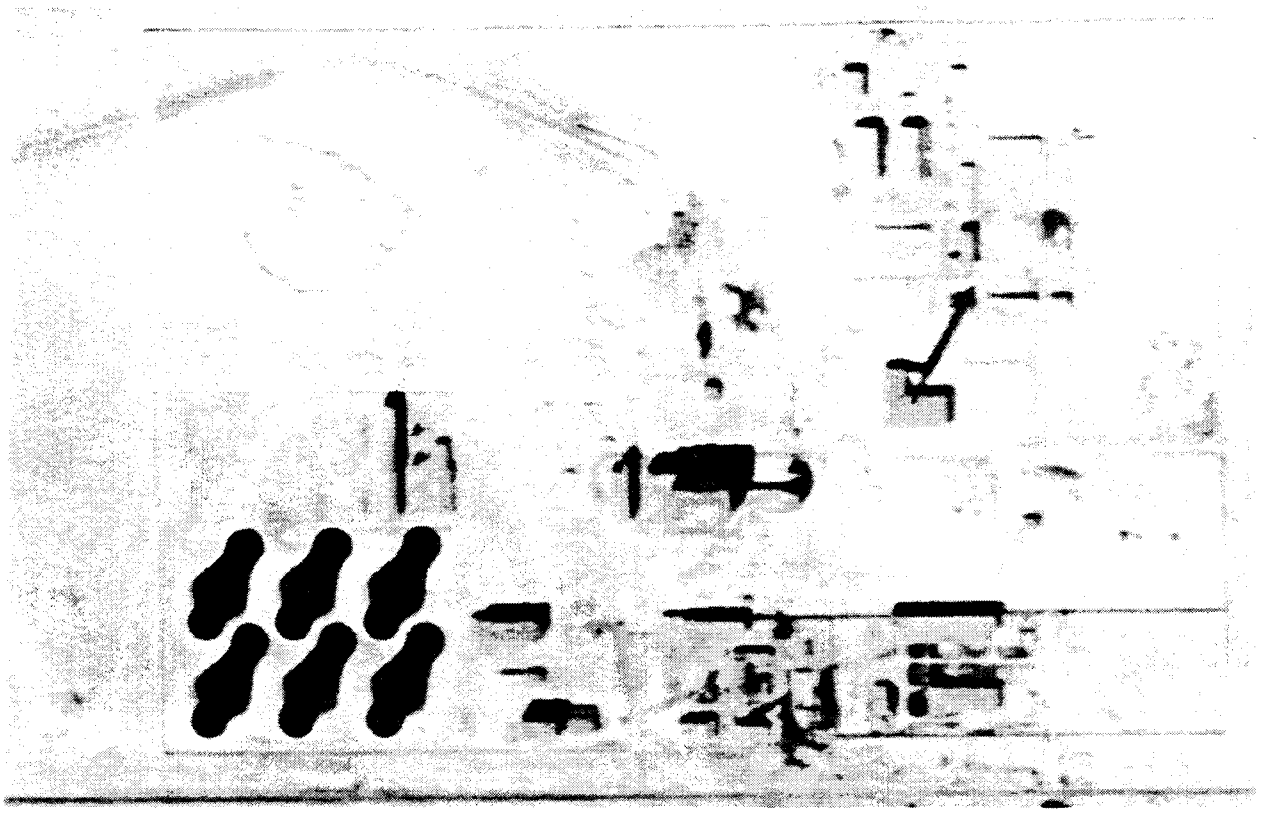

Fig.13b Declassified U.S. Corona Satellite Image of Jiuquan Reactor.
(Mission 1101-1, 18 September 1967, KH-4B system with 6 ft (1.8m) spatial resolution).
Comparing with Fig.12a, it is clear to see that all the towers been completed.

Conclusion

We conclude that whether or not a production reactor is operating can be monitored effectively using commercial observation satellites with high spatial resolution VNIR images complemented by lower-spatial resolution but good temperature resolution TIR images. These satellites can also be useful for the detection of undeclared nuclear-reactor sites and suspicious construction activities. Therefore, the new generation of commercial observation satellites could play a valuable role in the verification of an FMCT or a cutoff moratorium. Unlike information obtained by U.S. and Russian observation satellites, the information from commercial satellites could be available to all parties and to NGOs as well.

According to the legal regime of the Outer Space Treaty of 1967(OST), satellites for verification are protected by the understanding that outer space is open to all nations or groups to be used for peaceful purposes.[45] Consequently, the use of observation satellites used for verifying multilateral agreements is politically acceptable and technically feasible. There is the potential concern that a nation could enter into an exclusive arrangement with the operator of a commercial satellite to buy all images of its sensitive sites so as to deny these images to other organizations. However, given the number of competing 1-m resolution systems that are being launched (see Tables 2 and 3), it appears unlikely that one nation could make such arrangements with all the operators. In the future, however, to minimize such political issues, an international verification agency could own one or more dedicated observation satellites.[46]

ACKNOWLEDGEMENT

The authors would like to thank Harold A. Feiveson of the Center for Energy and Environmental Studies at Princeton University for his very helpful comments on this work. The authors also thank all those who provided information relating this work.

---

[45] U.S. Arms Control and Disarmament Agency, Arms Control and Disarmament Agreements: Texts and Histories of the Negotiations,1996 edition.

[46] Hui Zhang, "A View on the Application of Overhead Imagery to strength the IAEA Safeguards Regime," in Arms Control and The Rule of Law: A Framework for Peace and Security in Outer Space,ed.J.Beier and S.Mataija, (York University,Toronto1998).

Appendix A. The evolving capabilities of commercial observation satellites

Soon after the USSR and USA launched their first satellites (Sputnik-1 in Oct.1957 and Discover-1, in Feb.1959), they developed military reconnaissance satellites which were used as well starting in 1972 with SALT-I and the ABM Treaty as "National Technical Means" (NTM) to verify strategic arms control agreements. At the same time, lower resolution observation satellites were made available for civilian purposes, starting with the launch of U.S. Landsat-1 in 1972, whose spatial resolution in the visible spectrum is 80m.[47]

In 1986, international competition in the satellite imaging began with the launch by France of SPOT-1 with a resolution of 10m. In 1987, the USSR began marketing imagery from its KVR-1000 with a resolution down to 5m. France launched SPOT-2 in 1990 and SPOT-3 in 1993 (which failed on Nov.14, 1997), and SPOT-4 is scheduled for launch soon –all with a resolution of 10m. SPOT-5, scheduled to be launched in 2002, will have a resolution of 3m. In the meantime, India's IRS-1C and IRS-1D were successfully launched into orbit, in December 1995 and September 1997 respectively, each with a resolution of 5.8m.[48]

In December 1997, the U.S. firm, EarthWatch, launched EarlyBird into orbit with a spatial resolution of 3m -- but soon it failed. Recently, Russia SPIN-2 (Space Information - 2 meters) began to provide 2-m resolution images dating back to 1980, the highest resolution images available commercially at this moment.[49] However, since its images are acquired on photographic film, which is delivered back to Earth inside a reentry vehicle after a typically 28-day mission, customers must usually wait for a considerable time to get new images and cannot regularly revisit the same site. Moreover, the satellite orbit differs from those of other commercial satellites in that it is not sun-synchronous, near-polar.

On March 9,1994, the U.S. Government decided to allow U.S. companies to build and launch private observation satellites that could obtain imagery with one-meter or better resolution.[50] On April 27, 1999, the U.S. firm, Space Imaging, launched the first such satellite, IKONOS, with a 1-m-resolution panchromatic sensor and a 4m-resolution multispectral sensor.

---

[47] T.M. Lillesand and R. Kiefer, Remote sensing and image interpretation, (John Wiley & Sons, Inc, 1994).
[48] See http://www.euromap.de/
[49] See http://www.spin-2.com/
[50] U.S. White House, "Fact sheet on U.S. policy on foreign access to remote sensing space capabilities,"

However, the satellite failed soon after launch. The U.S. firm EarthWatch plans to launch QuickBird in late 1999.[51] The satellite will carry a 1-m resolution panchromatic sensor and a 4-m resolution multispectral sensor with blue, green, red and near infrared, so it can get true color images from spaces. The U.S. Company Orbimage also plans to launch the Orbview-3 satellite this year with 1-meter panchromatic and 4-meter multispectral digital imagery.[52] Finally, the Israel firm, West Indian Space (WIS), is planning to launch and operate a constellation of high resolution commercial imaging satellites, the EROS (Earth Remote Observation System) starting in late 1999, with the EROS-A satellite with 1.8-meter resolution, followed in 2001by EROS-B with an 0.8-meter resolution.[53]

In addition to 1-m resolution, all these new-generation commercial observation satellites have: relatively short revisit intervals (1-5 days); fore-and aft and side to side pointing capability, as well as stereo imaging; huge on-board data storage capacity; and image delivery times to customers of hours to days.

Technical considerations

Spatial resolution and object identification. The smaller the resolution the more details are visible in an image. For photographic film the most common definition is based on the number of equidistant dark bars in a standard resolution target which can be resolved per millimeter of film. Approximately one line-pair is necessary to detect an object. The spatial resolution definition used in this paper is that used for electro-optical sensors, the size of the smallest area sampled by the system detector element, a "pixel", projected onto the ground. This is referred to as the "instantaneous field of view" (IFOV). This depends on not only the characteristics of the detector and of the optical system, but also the orbit height and the wavelength of the radiation to be detected. Approximately two pixels are required to present the same amount of ground information as one line pair at 'normal' film contrast. In addition, spectral resolution across a range of wavelengths is useful for separating objects of different composition but similar reflectance.

Revisit time. For timely detection of clandestine nuclear activities, short revisit times to

---

March10,1994,p.1.

[51] See http://www.digitalglobe.com

[52] See http://www.orbital.com

[53] See http://www.westindianspace.com/

specific geographic points are helpful. Revisit times are dependent upon the flight parameters of the satellites and the width of the swath viewed by the sensor. Ability to point to the left and right of the satellite can also decrease the revisit time significantly. Oblique imaging can also be used to acquire stereo pairs to facilitate object identification. It is preferable, however, to acquire a stereo pair in a single orbital pass through fore and aft viewing.

Satellite orbits. Earth observation satellites typically operate in circular or slightly elliptical orbits, giving them almost constant resolution worldwide. High-resolution satellites operate in the height range 100-1000 km. with corresponding orbital periods between of 85-105 minutes. The angle between the orbit plane and the equatorial plane, the "inclination", defines the latitudes that can be observed. In order to cover the whole earth an inclination of about 90° is usually chosen. Since comparison of images of a given location acquired on different dates depends on similarity of the conditions of illumination, the orbital plane is also chosen to be sun-synchronous so that the satellite overflies any given point at the same local time.

Appendix B. The lengths of vapor plumes from wet cooling towers

In wet cooling towers (both natural-draft and mechanical-draft), the primary cooling mechanism is evaporation. Hot water is dripped through the packing in the bottom of the tower as air flows upward through it.[54] Usually the design of the cooling tower results in the air being almost saturated when leaving the pack. The amount of water evaporated per kilogram of air passing through therefore depends upon the "wet-bulb" temperatures of the air entering and leaving the packing. The wet-bulb temperature is the temperature at which air carrying a given percentage of water would be saturated. The wet-bulb temperature of the entering air therefore determines how much water it is carrying in and that of the exiting air how much is being carried out.

As the air rises it expands and cools. As a result condensation of water occurs, resulting in a visible plume almost always being present.[55] After the plume leaves the tower, its buoyancy will lead to its continued rise.[56] It will also mix with the ambient air. How far downwind the resulting mixture will remain supersaturated depends upon the saturation level of the ambient air. Figure B-1, a "psychometric chart"[57] showing the grams of water vapor per m^3 of saturated air as a function of temperature, makes it simple to illustrate this fact. Point o in the figure corresponds to the slightly supersaturated state of air leaving a cooling tower at a temperature of about 25 °C. Pont i represents the state of the intake air (ambient atmosphere)at about 8 °C and 70 percent saturation. All mixtures of effluent air from the cooling tower system and ambient air will lie along the line oi. The intersection point c is usually named critical dilution point. In the region of the diagram between the o and c, the air mixture is supersaturated, condensation

---

[54] N.P.Cheremisinoff,et al., Cooling Towers: Selection, Design and Practice,(Ann Arbor Science Pulishers,Inc.,1981); W. Stanford and G. Hill, Cooling Towers: Principle and Practice, (Carter Industrial Products Limited, England, 1972); R. Woodson, "Cooling Tower", Scientific American, May1971; W.Maze, "Practical Tips on Cooling Tower Sizing", Hydrocarbon Process, No.2,1967.

[55] F.R. Barber, et al., "The persistence of plume from natural draught cooling towers," Atmo.Envir.,Vol.8,pp407,1974. Atmospheric pressure decreases by about 1 percent per hundred meters at sea level. For unsaturated air, the temperature would therefore decline by about one percent or about 3 °K. However, the condensation of water vapor could offset this effect. At 30 °C, for example, cooling by 3 °C would reduce the amount of water that could be carried by a kg of saturated air by 4 grams, which would release 10 kj of heat -- enough to raise the temperature by 10 °C. The net result would therefore be to reduce the cooling for saturated air to about 0.7 °C.

[56] G.Csanady, "Bent-Over vapor plumes, " J.Appl.Meteor.,1971,Vol.10.,p.36

[57] Cooling tower plume modeling and drift measurement, (The American Society of mechanical Engineers, New York, 1975).

will occur and the plume will therefore be visible. Beyond the plume becomes undersaturated and the plume will disappear. If the ambient air is already saturated, the visible plume will, in principle, extend indefinitely.

To estimate the length of the visible plume, the critical dilution ratio (R_d), the ratio of the final to the initial volume of humid air, can be determined from the psychometric chart as

$$R_d = (T_o - T_i)/(T_c - T_i) \qquad \text{(B-1)}$$

where T_o ,T_c and T_i are the temperatures of air at the points o, c, and i. T_o depends the ambient temperature and humidity and the amount of cooling per kg of air passing through the cooling tower.

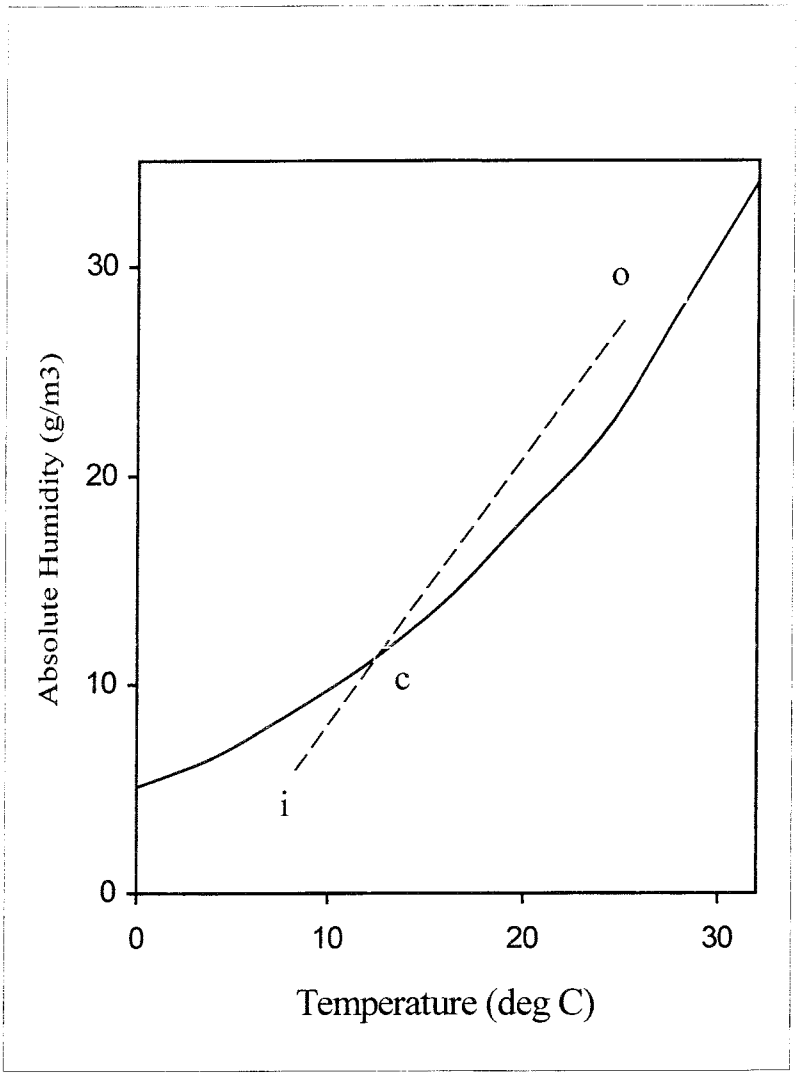

Fig B-1 A Simplified Psychrometric Chart Illustrating the Saturation Absolute Humidity versus Temperature.
The solid line represents the saturation line. A state on the left of the saturation line is supersaturated; and on the right is unsaturated.

Temperature increase and velocity of air discharged from a Natural-draft cooling tower. The enthalpy of vaporization of a kg of water is about 2.4 Mj and the specific heat of a kg of air is 1 kJ per °C. The flux of energy removal (MWth) per m^2 of exit aperture at the top of the cooling tower is therefore

$$p = jx[0.001x(T_o - T_i) + 2.4\,(F_0 - F_i)]\ \ MWt/m^2 \qquad (B\text{-}2)$$

where and F_i and F_o are the water vapor mass fractions in the incoming and outgoing air, $\Delta T \equiv T_o - T_i$, is the temperature difference between the incoming and outgoing air, and j is the mass flux of air through the cooling tower aperture in kg/m^2-sec

$$j = \rho_o V_o \qquad (B\text{-}3)$$

where ρ_o is the mass density of the exiting air (kg/m^3) and V_o is its velocity.

In a natural-draft cooling-tower, the gas exit velocity is determined by the density difference ($\Delta\rho$) between the air inside and outside the cooling tower and the cooling tower height (h in meters)[58] according to the energy-conservation formula

$$(1/2)\rho_o V_o^2 = K*\Delta\rho*g*h \qquad (B\text{-}4)$$

where $g = 9.8$ m/sec^2 is the gravitational constant and K is a factor less than one representing the reduction in available potential energy due to dissipative losses in the packing and elsewhere in the tower.[59] Then, using the perfect gas law and neglecting the change in average molar mass between the incoming and outgoing air due to the addition of water vapor, we can also approximate

$$\Delta\rho/\rho_o = \Delta T/T_i \qquad (B\text{-}5)$$

---

[58] Typical about twice the top diameter .

[59] The static pressure losses of the air as it flows through the tower are mainly for the packing which represent about three-fourths of the overall pressure loss. Here it is assumed that K is about 1/4. See also Handbook of Energy Systems Engineering: Production and Utilization, ed. L. Wilbur,et al., John Wiley&Sons.

Eqn. B-4 then becomes

$$V_o^2 = (2K)\,(\Delta T/T_i)*g*h. \qquad \text{(B-6)}$$

This gives

$$V_o = 0.9C_s[\Delta T]^{1/2} \qquad \text{(B-7)}$$

where the scaling factor

$$C_s = [(4K)(h/50)(300/T_i)]^{1/2}$$

equals 1 when K = 1/4, h = 50 m. and T_i = 300 °K.

Substituting (B-3) and (B-7) in (B-2) and approximating $\rho_o \approx 1$ kg/m^3 then gives

$$p = 1.28C_s\,(\Delta T)^{1/2}\,[0.001\Delta T + 2.4\,(F_o - F_i)]\ \text{MWt/m}^2 \qquad \text{(B-8)}$$

The fraction of water by weight carried by saturated air as a function of temperature may be approximated from 0-30 °C as

$$F_w^{\,s}\,(T) = [3.7448 + 0.365118T - 0.0016594T^2 + 0.00047455T^3]\text{x}10^{-3} \qquad \text{(B-9)}$$

where T is the temperature in °C . In B-8, therefore, $F_o = F_w^{\,s}\,(T_O)$ and $F_i = f_i\text{x}\,F_w^{\,s}\,(T_i)$, where f_i is the fractional saturation of the incoming air.

Consequently, given the flux of energy removal (MWth) per m^2 of exit aperture at the top of the cooling tower, the temperature and velocity of air leaving a cooling tower can be estimated from Eqn.B-7 and 8.

Figure B-2 shows a plot of p against ΔT for h= 60m , K=1/4, and for f_i = 0,1, and for T_i = 0, 10, 20, 30 °C. For the case of the Tomsk-7 cooling towers: assuming each tower has a cooling capacity of 200MWt, then the flux of energy removal is about 0.3 MWt/m^2. Then from figure

B-2, it will be seen that, for an ambient air temperature of 20 °C and 50 percent humidity, the temperature increase of the discharged plume is about 14.5 °C. Based on Eq.(B-7), It can also estimate that the velocity of air leaving the towers is about 4m/s.

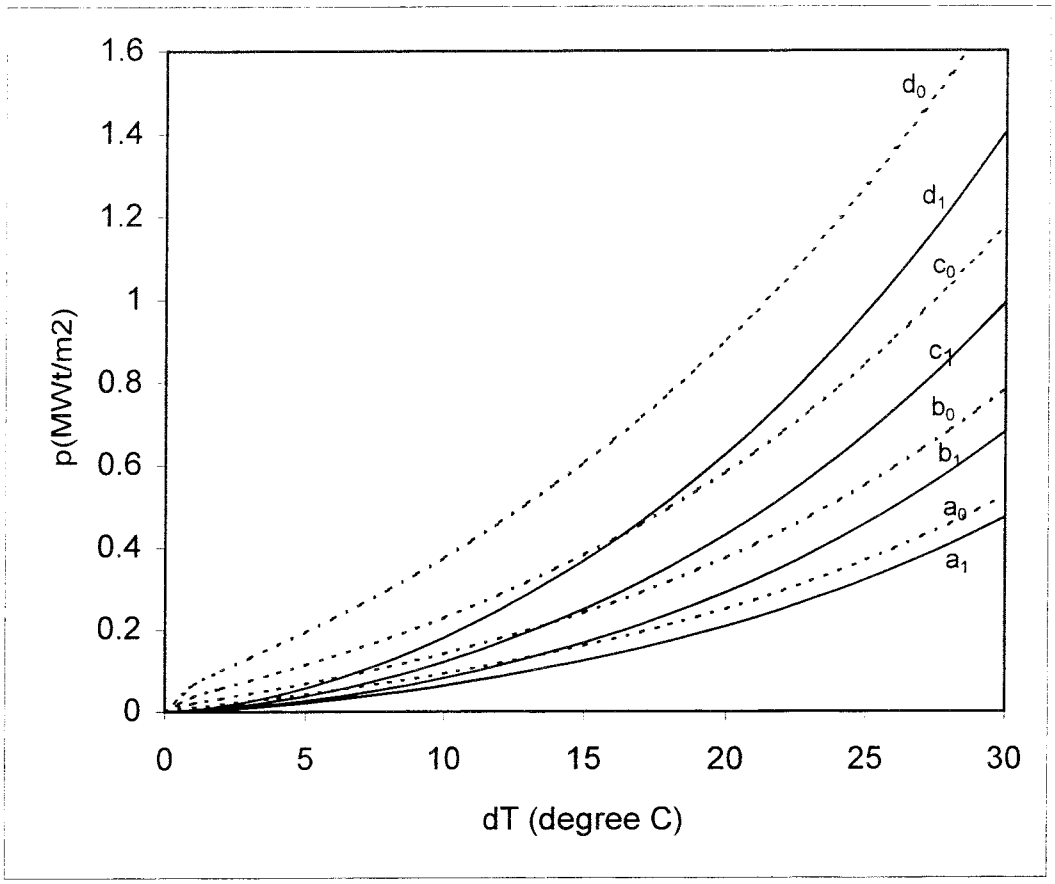

Fig.B-2 The flux of energy removal(MWt) per m^2 versus the temperature increase.

(line a_0: T_i=0°C, f_i=0; a_1: T_i=0°C, f_i=1; b_0: T_i=10°C, f_i=0; b_1: T_i=10°C, f_i=1;
c_0 :T_i=20°C, f_i=0; c_1 : T_i=20°C, f_i=1; d_0: T_i=30°C, f_i=0; d_1 :T_i=30°C, f_i=1)

Plume dispersion. The most common approach to model plume mixing assumes Gaussian dispersion with different dispersion coefficients for the horizontal and vertical directions. The water concentration is given by

$$\chi(x,y,z)=\frac{Q}{2\pi u\sigma_y\sigma_z}\exp(-\frac{y^2}{2\sigma_y})[\exp(-\frac{(z+H)^2}{2\sigma_z^2})+\exp(-\frac{(z-H)^2}{2\sigma_z^2})] \qquad \text{(B-10)}$$

Where χ is the mass concentration of water; Q is the emitted mass flux of water; x is the downwind distance from the tower; y is the horizontal distance from the plume center line, z is the perpendicular to x and y (perpendicular to the earth's surface if the plume is horizontal), and σ_y and σ_z, which are functions of x, are measures of the plume's horizontal and vertical growth as it drifts σ_y and σ_z are the standard deviations of water concentration in the cross-wind and vertical directions ; [60]H is the height of the plume centerline (which may be a function x if the buoyancy of the plume causes it to rise);u is the mean wind speed.

The dispersion parameters, σ_y and σ_z, grow with downwind distance x in a fashion that depends upon atmospheric conditions in the lowest "mixing layer. These conditions vary from extremely unstable (as, for example, in the afternoon of a bright sunny day when the earth is warmer than the atmosphere and therefore generates rising "thermals") to extremely stable (as early in the morning after a clear night, when the ground is cooler than the air above). Pasquill has divided these stability conditions into 6 classes, A-F, with A being the most unstable and F being the most stable and various modelers have offered empirical functional forms of σ_y and σ_z for each stability category. Here we use the analytic forms given by Green et al.[61] as follows,

$$\sigma_y(x)=\frac{k_1 x}{(1+\frac{x}{k_2})^{k_3}} \qquad \text{(B-11)}$$

[60] See e.g.D Bruce Turner, Workbook of Atmospheric Dispersion estimates: An Introduction to Dispersion Modeling, (CRC press, 1994).

[61] A.Green,et al., "Analytic extensions of the Gaussian plume Model," JAPCA, Vol.30, No.7,1980.

$$\sigma_z(x) = \frac{k_4 x}{(1 + \frac{x}{k_2})^{k_5}} \quad \text{(B - 12)}$$

Where k_1-k_5 are constants dependent on the atmospheric stability(see table B-1).

Table B-1. k values in Eqn.B-11 and 12.

atmospheric stability	k_1	k_2	k_3	k_4	k_5
A	0.250	927	0.189	0.1020	-1.918
B	0.202	370	0.162	0.0962	-0.101
C	0.134	283	0.134	0.0722	0.102
D	0.0787	707	0.135	0.0475	0.456
E	0.0566	1070	0.137	0.0335	0.624
F	0.0370	1170	0.134	0.0220	0.700

Based on Eq.(B-10), the water concentration along the plume centerline (i.e. y=0, z =H) is given by

$$\chi = \frac{Q}{2\pi u \sigma_y \sigma_z}\left[1 + \exp(-\frac{1}{2}(\frac{2H}{\sigma_z})^2)\right] \quad \text{(B - 13)}$$

In addition, the initial concentration of water at the cooling tower exit is given by,

$$\chi_0 = \frac{Q}{\pi R^2 V_0} \quad \text{(B - 14)}$$

Where R_0 is the radius of the tower exit; V_0 is the exit velocity of the tower effluent.

Combining Eqn.B-13 at the source and B-14, then

$$\sigma_y^0 \sigma_z^0 = \frac{R^2 V_0}{2u} \quad \text{(B - 15)}$$

Where σ_y° and σ_z° are the initial values of σ_y and σ_z at the plume, i.e. x_o. We assume that $\sigma_y^\circ = R/(2)^{1/2}$, then $\sigma_z^\circ = (V_0/u)(R/(2)^{1/2})$.

Using B-13, for distances downwind shorter than that at which σ_z° becomes comparable to the distance of the plume from the ground or the top of the "mixing layer," the dilution ratio along the plume centerline is given by

$$\frac{\chi_0}{\chi} = \frac{\sigma_y \sigma_z}{\sigma_y^0 \sigma_z^0} \quad \text{(B - 16)}$$

For cases such as the present one, where $\sigma_y(0)$, $\sigma_z(0)$ are already of significant size, x is replaced by $x + x_y$ or $x + x_z$ so that $\sigma_y(0)$ and $\sigma_z(0)$ have the appropriate initial values. Consequently, based on B-16, the ratio χ_0/χ can be determined by the method of virtual sources. When this ratio falls to R_d, the centerline concentration falls below saturation and the plume disappears.

As an example, we still consider the case for the cooling towers of Tomsk-7 reactors. Assume that 1) the cooling capacity of each tower is 0.3 MWth/m^2; 2) the tower height (h) is 60m (about twice the tower diameter(30m); 3) the average windspeed is 4m/s; 4) the plume temperature at the tower top is 1 ^{0}C lower than that of leaving the pack.[62]

Considering the ambient air temperature of 20 ^{0}C and 80 percent humidity, based on the Eq.(B-8) , B-9, Fig.B-1,and Eq.(B-1), then the critical dilution factor is estimated about 4 at the end of the visible plume. Furthermore, for different weather class A, D and F, based on Eq.(B-16), B-10,B-11 and B-12, the horizontal cross-section of the visible plume through the plume central line can be estimated as shown in figure B-3. It shows that the length of the visible plume is approximately 50m, 200m and 500m for weather class A,D and F respectively. In fact, the size of the visible plume depends not only on the weather stability, but also on other factors such as the relative humidity of the ambient air. For example, for the same cooling tower

performance and the weather state as above except the relative humidity 50 percent, then the length of the visible plume would reduce to 20m,80m and 200m for weather class A,D and F respectively.

Finally, based on the above discussion, we can estimate the size of the visible plume from the wet-type cooling towers for various weathers and operating condition. Consequently, it could be concluded that: under almost all weather and operating conditions of the towers, a plume of condensed water is visible at least at the exit of the cooling tower. With low relative humidity and high air temperature, such plumes are short and quickly dispersed. However, during periods of low wind speed, and high humidity or low air temperature, the plumes may be very dense and can extend for several kilometers downwind before disappearing.

---

[62] See ref.55.

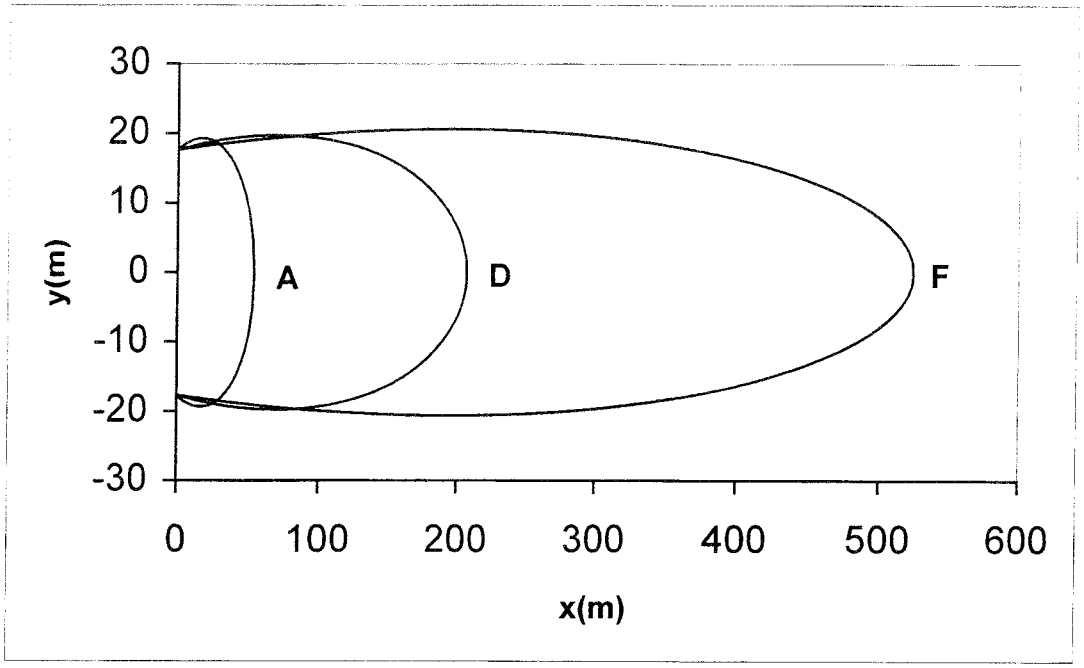

Fig.B-3 Horizontal cross-sections of the visible plume through the plume central line for a Tomsk-7 tower: point(0,0) is the location of the tower top, x is the downwind distance; y is the horizontal distance from plume center line; windspeed 4m/s, Pasquill-class A, D, F, ambient air temperature 20 ^{0}C, relative humidity 80%.

Appendix C. Detectability with TIR sensors of objects smaller than the instantaneous field of view of a pixel

A black body radiates a total energy flux of $S= \sigma T^4$ in Watts per m^2 where; σ is Stefan-Boltzmann constant (5.67×10^{-8} Watts/(m^2-$^oK^4$) and T is the absolute temperature of the warm plume. Then the total power from a black body with area (A) is:

$$P=\sigma T^4 A \qquad \text{(C-1)}$$

If A is smaller then the instantaneous field of view of a pixel (A_p) of a satellite TIR detector, it will raise the effective temperature seen by the detector according to an area-weighted average with the background temperature:

$$\sigma T^4 A+\sigma T_b^4 (A_p-A)=\sigma T_{eff}^4 A_p \qquad \text{(C-2)}$$

where T_b is the ambient temperature .

Solving C-2 for values of $T - T_b$ small in comparison with the absolute temperature T gives

$$\Delta T_{eff} \equiv T_{eff}-T_b \approx (T-T_b)(A/A_p) \qquad \text{(C-3)}$$

In order to be detectable, ΔT_{eff} must be greater than the threshold sensitivity of the TIR detector, ΔT_{th} or

$$A(T-T_b) \geq A_p T_{th} \qquad \text{(C-4)}$$

As an extreme example consider the detectability of vapor plumes if they were visible only inside the tops ot the Tomsk-7 reactor cooling towers – as nearly appears to be the case for some of the Tomsk-7 cooling towers in Fig. 3. The inside diameter of each tower top at the Tomsk-7 reactor site shown in Fig. 3 is approximately 30m. From the declassified Corona satellite image as shown in Fig.12b, it can be estimated that the inside diameter of each tower top at the Jiuquan reactor site is approximate 20m. Based on the ratings of the associated

production reactors, the Tomsk-7 cooling towers must have a cooling capacity of at least 200 MWt or 0.3 MWt/m^2. For an ambient air temperature of 20 °C and 50 percent humidity, this would require a temperature difference between the input and output air of the cooling tower of about 14.5 °C (see Appendix B). The area of a single tower top is about 700 m^2. If the ground temperature is also 20 °C, therefore, $A(T-T_b) \approx 10^4$ m^2-°C. Similarly, for Jiuquan reactor, the area of its single tower top is about half that of Tomsk-7, that is $A(T-T_b)$ is about 5,000 m^2-°C, For comparison, according to Table 3, A_pT_{th} for the TIR detectors on Landsat-5, 7 and Aster are: 7-14,000, 2-4,000, and 1,600 m^2-°C respectively. It therefore appears that, even if a plume does not cover an area bigger than the top of a Tomsk-7 cooling tower or a Jiuquan cooling tower, it should be detectable by the TIR detectors on Landsat-7 and Aster. However, the detection of the TIR detector on board Landsat-5 would depend on effective size of the plume , the elevated temperature leaving the towers and the ambient air condition etc.

Appendix D. Sizing Cooling Ponds[63]

For a given surface area, the most efficient cooling pond is deep enough to allow density currents to spread the warm water effluent efficiently over the surface of the pond. The water inlet should be located at the coolest point of the pond surface , and there should be minimal mixing of the hot water with the cooler deep water to ensure the warmest surface layer temperature possible for highest surface cooling.[64] The time required for water to pass through the pond depends on the rate of pumping and the pond volume while the temperature drop from the plant discharge to the plant intake depends on the rate of pumping and the pond surface area. Since the water surface temperature varies with distance from the discharge point, the heat transfer rate from the pond surface is not uniform.

The heat transfer rate from the pond surface is

$$P = \int K(T_s - T_e)dA \ \text{Watts} \qquad \text{(D-1)}$$

where K is the surface heat exchange coefficient in Watts/m^2-°C, A= pond surface area in m^2, and T_s and T_e are respectively the local and equilibrium surface temperatures in °C.

The equilibrium temperature is the water surface temperature at which there is no net heat transfer from the water surface to the atmosphere and (by radiation) space. The surface heat exchange coefficient depends on the wind speed, temperature and wet-bulb temperature (T_{wet}) of the air above the pond and has been parameterized as follows:[65]

$$K = 3.7 + 3.97(1 + 0.05V^2)(1.04 + 0.761T' + 0.0026T'^2) \ \text{W/m}^2\text{-°C} \qquad \text{(D-2)}$$

where V is the wind velocity in m/sec and $T'=(T_s+T_{wet})/2$. The surface heat exchange

---

[63] K.W.Li and A.Priddy, Power Plant System Design, (John Wiley &Sons,1983);G.Jirk,et al.,"Steady State Estimation of Cooling Pond Performance," J.Hydraulics Division,ASCE 106(HY6),June 1980.

[64] G.H.Jirka,et al.,"Cooling Impoundments: Classification and Analysis," J.Energy Division, Vol.105,No.EY2,Aug.1979. The wet-bulb temperatureT_{wet} is determined implicitly by the air temperature T_{air} and fractional humidity f_{air} as $T_{wet} = T_{air} - 2400[(1 - f_{air}) F_w^s (T_{air}) - F_w^s (T_{wet})]$, where $F_w^s (T)$, the fractional weight of water in saturated air, is given by equation(B-9).

[65] D.K.Brady,et al., "Surface Heat Exchange in Power Plant Cooling Lakes," research report, Hohn Hopkins

coefficient generally ranges between 20-40 Watts/m^2-^{0}C.[66]

In a steady-state, steady-flow condition this heat dissipation rate is equal to the difference between the heat into the pond and the heat out of the pond. In terms of the plant intake and discharge temperature, it is

$$P = C_w \rho J_w \Delta T \quad \text{Watts} \tag{D-3}$$

where ρ is the water density (1000 kg/m^3), C_w is the specific heat of water (4200 j/kg-°C), J_w is the water flow rate in m^3/sec, $\Delta T = T_d - T_i$ and T_d and T_i are respectively the water discharge and intake temperatures (°C). For ΔT = 15 °C, J_w = 16 (m^3/sec)/GWth.

Given a steady-state, steady-flow condition, one can equate (D-1) and(D-3

$$C_w \rho J_w (T_d - T_i) = \int K(T_s - T_e) dA \tag{D-4}$$

One can also apply this same equation to the water flow through and the heat loss rate from a strip of the surface of the pond with an average temperature T_s and a temperature difference dT_s between its upstream and downstream sides to get the differential equation

$$C_w \rho J_w dT_s = K(T_s - T_e) dA \tag{D-5}$$

D-5 has the solution $\ln [(T_d - T_e)/(T_i - T_e)] = KA/(C_w \rho J_w)$ (D-6)

Combining D-6 and D-1 gives the pond area per MWth required to achieve a given cooling ratio

$$r \equiv (T_d - T_e)/(T_i - T_e)$$

as $$A/P = \ln r/K = (\ln r)/[K(T_d - T_i)] \quad km^2/MW. \tag{D-7}$$

University Press,1969; K.W.Li and A.Priddy, Power Plant System Design,(John Wiley&Sons,1983).

[66] D.K.Brady,et al.,"Surface Heat Exchange in Power Plant Cooling Lakes," Research Report,Johns Hopkins University Press,1969.